Bulletin of the Seismological Society of America, Vol. 101, No. 4, pp. 1783–1806, August 2011, doi: 10.1785/0120100285

A Model for Vertical-to-Horizontal Response Spectral Ratios for Europe and the Middle East

by Julian J. Bommer, Sinan Akkar, and Özkan Kale

Abstract In the framework of probabilistic seismic hazard analysis, the preferred approach for obtaining the response spectrum of the vertical component of motion is to scale the horizontal spectrum by vertical-to-horizontal (V/H) spectral ratios. In order to apply these ratios to scenario or conditional mean spectra, the V/H ratios need to be defined as a function of variables such as magnitude, distance, and site classification. A new model for the prediction of V/H ratios for peak ground acceleration and spectral accelerations from 0.02 to 3.0 s is developed from the database of strong-motion accelerograms from Europe and the Middle East. A simple functional form, expressing the V/H ratios as a function of magnitude, style of faulting, distance, and site class, is found to be appropriate, and the associated aleatory variability is found to be at least as low as that obtained in other studies using more complex models. The predicted ratios from the new European model are found to be in broad agreement with recent models derived from predominantly western North America data.

Introduction

Lateral loads imposed on structures are the primary cause of damage in earthquakes, but the vertical component of ground shaking can also contribute to the destructive capacity of the motion in many situations. For consideration of such cases, and for modeling the interaction between the horizontal and vertical components of the ground motion, it is necessary to define the input to structural design in terms of both vertical and horizontal accelerations. The reader is referred to Bozorgnia and Campbell (2004a) for the significance of vertical ground motions in engineering design applications. When generating design response spectra through probabilistic seismic hazard analysis (PSHA), one option is to repeat the hazard integrations conducted in terms of horizontal response spectral ordinates using ground-motion prediction equations (GMPEs) for the vertical spectral ordinates. The problem with such an approach is that, if the hazard at a particular response period is subsequently disaggregated for a given annual exceedance frequency, it may often be found that the vertical and horizontal spectral accelerations are controlled by different earthquake scenarios. This shortcoming becomes particularly important if three-component acceleration time-histories are subsequently required for dynamic structural analyses. The preferred approach, therefore, is to generate the vertical spectrum by multiplying the horizontal spectrum by vertical-to-horizontal (V/H) ratios.

Such V/H ratios can be applied to the uniform hazard spectrum (UHS), to a scenario spectrum, or to a conditional mean spectrum (CMS) (Baker and Cornell, 2006), as discussed by Gülerce and Abrahamson (2011). The CMS, in effect, is a special case of the scenario spectrum that accounts for the decreasing correlation of the variability of spectral ordinates with increasing separation of response periods. The first option (UHS) has two important shortcomings, the first being that the UHS is not a suitable target for the selection and scaling of accelerograms (e.g., Thenhaus and Campbell, 2002), and the second that generic rather than scenario-specific V/H factors would need to be used. The latter options of applying V/H ratios to a scenario spectrum or CMS are preferable, but they require models for predicting V/H ratios as a function of the explanatory variables that characterize the controlling earthquake scenario and the site of interest. Therefore, as a minimum, such a model should include the influence of earthquake magnitude, source-to-site distance, and site class; style of faulting may also be a relevant parameter.

Another point that should be noted regarding such models is that the vertical component of ground motion tends to be most pronounced at short response periods, and vertical vibration modes of structures tend to have much shorter periods than do modes of horizontal vibration. Therefore, models for V/H spectral ratios should ideally be derived for a wide range of response periods and in particular to provide good coverage of the short-period range of the response spectrum.

For application to a UHS or to a scenario spectrum, only the median values of the V/H ratios are required. This makes the implicit assumption that the aleatory variability associated with the prediction of the vertical component is equal to that associated with the horizontal component, whereas

the results of some studies suggest that the former might actually be slightly larger (Campbell and Bozorgnia, 2003). For the most accurate generation of vertical spectra, Gülerce and Abrahamson (2011) propose applying the V/H ratios to the CMS and additionally adjusting for the period-to-period correlation between the horizontal spectral ordinates and the V/H ratios. This approach requires a measure of the variability of the predicted V/H ratios, so this becomes another requirement for these models.

Despite the clear need for V/H spectral ratio models, relatively few have been presented in the literature, and there are important shortcomings with some of the existing models. In the next section, models for the V/H ratios of response spectral ordinates are reviewed, after which we present the generation of a new V/H model using the current European strong-motion database.

Models for V/H Response Spectral Ratios

The existing models for predicting the V/H ratio of response spectral ordinates can be grouped into three categories: (1) codes and regulations, which present generic ratios that usually vary only as a function of site classification; (2) independent predictions of the vertical and horizontal components of motion, which allow the median V/H ratio to be calculated for a given scenario; and (3) direct predictions of the V/H ratio, which have the advantage of generally including a measure of the associated variability. The currently available models in each of these three categories are reviewed in the following three subsections.

V/H Ratios from Codes and Regulations

Many seismic design codes do not consider the vertical component of motion at all, and, among those that do specify a vertical response spectrum, it is not uncommon for this to be specified simply as 2/3 of the horizontal spectrum at all response periods. There are, however, a few code-specified vertical spectra that more realistically reflect the variation of the V/H ratio with response period. The earliest of these is Regulatory Guide (RG) 1.60 (United States Atomic Energy Commission [USAEC], 1973), in which the V/H spectral ratio is equal to 2/3 for frequencies of less than 0.25 Hz but equal to 1.0 for frequencies above 3.5 Hz. McGuire *et al.* (2001) proposed updates intended to replace the RG 1.60 spectra, for which they put forward distinct V/H spectral shapes for the western United States and for central and eastern United States. These ratios are defined for rock sites and vary with the range of expected peak ground acceleration (PGA) value in rock, as a surrogate for capturing the influence of magnitude and distance.

Eurocode 8 (2004) was among the first codes for the seismic design of buildings to include a vertical spectrum defined independently from the horizontal spectrum, based largely on the proposed V/H model of Elnashai and Papazoglu (1997). The National Earthquake Hazards Reduction Program [NEHRP] (2009) provisions have similarly introduced an independent specification of the vertical spectrum, based in this case on the proposals of Bozorgnia and Campbell (2004b). Other recent proposals for simple V/H spectral ratios include those of Malhotra (2006) and Cauzzi and Faccioli (2008). Figure 1 compares the implied ratios from EC8 and NEHRP (2009) with other simplified models. Figure 1a presents the V/H ratios embedded in these codes, as well as those proposed in the McGuire *et al.* (2001) study. Figure 1b plots include the empirical relationships of Cauzzi and Faccioli (2008) and Bozorgnia and Campbell (2004b), which is derived from the equations of Campbell and Bozorgnia (2003) that are discussed in the next section. The comparisons in Figure 1 clearly illustrate one of the key shortcomings of simplified V/H ratios such as those embedded in seismic design codes: they are generally unable to capture the strong influence of source-to-site distance. As noted previously in this paper, the approach of McGuire *et al.* (2001) to condition the V/H ratios to the rock PGA at the site, partially overcomes this problem. However, in general the use of such simplified V/H ratios is not ideal for site-specific applications. The main use of the generic V/H ratios encountered in design codes and regulations is to transform a horizontal UHS (approximated by the design spectrum) to a vertical UHS, for which little more than the site classification and the site-specific levels of motion will generally be known, unless a disaggregation is performed.

V/H Ratios from Independent Predictions of Spectral Ordinates

The V/H spectral ratio can be constructed for any earthquake scenario using independent GMPEs for the horizontal and vertical spectral ordinates, provided these are derived from the same dataset. We have identified 16 such pairs of predictive models in the current literature; their key characteristics are summarized in Table 1 in terms of the magnitude and distance ranges covered, as well as the range of response periods for which V/H ratios are provided (apart from PGA, which can be assumed as being equivalent to the spectral acceleration at 0.01 s).

Although included in Table 1, it should be noted that Bragato and Slejko (2005) used 3168 records for the vertical component model but only 1402 horizontal pairs for the equations to predict horizontal spectra, which means that the models cannot really be considered as compatible. Limitations with several of the other models in Table 1 are immediately apparent, with several of them being specific to individual countries or even subregions of countries. If we eliminate models for which the maximum magnitude considered is not greater than moment magnitude (M_w) 7 and those for which the minimum period covered is 0.10 s, 10 of the 16 models would be eliminated from further consideration.

From the six surviving models, Campbell (1997) can also be excluded because it has been superseded by

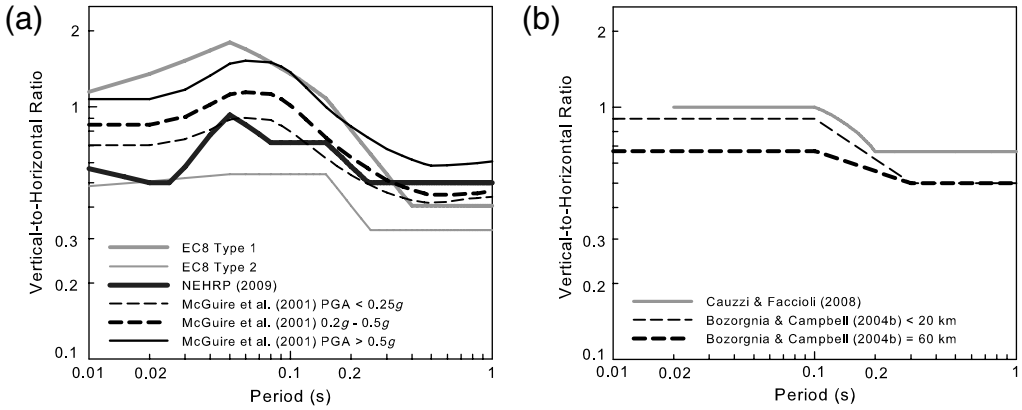

Figure 1. (a) Comparisons of V/H ratios from Eurocode 8 (EC8), NEHRP (2009), and McGuire *et al.* (2001) for western North America, for rock sites, compared with (b) those from Cauzzi and Faccoli (2008) and Bozorgnia and Campbell (2004b) for different distances. "Rock site" is taken as an NEHRP B site class definition for NEHRP (2009), whereas it is a Type A site class for EC8. Among the individual studies, Cauzzi and Faccioli (2008) define rock site conditions for $V_{S30} \geq 800$ m/s, and Bozorgnia and Campbell (2004b) consider the sites with $V_{S30} = 800$–330 m/s as rock.

Campbell and Bozorgnia (2003). Berge-Thierry *et al.* (2003) and Cauzzi and Faccioli (2008), while nominally applicable to larger magnitudes, have the disadvantage of being based on hypocentral distance (R_{hyp}), which is not an appropriate measure for larger events. Moreover, Berge-Thierry *et al.* (2003) only differentiates between rock and soil sites, without any additional refinement in terms of site classification.

This leaves just three models, two of which only extend down to 0.05 s (Ambraseys *et al.*, 2005a, 2005b; Campbell and Bozorgnia, 2003), with only Abrahamson and Silva (1997) including periods as short as 0.01 s. The Ambraseys *et al.* (2005a) model is for the larger horizontal component of motion, whereas ground-motion predictions are increasingly based on the geometric mean component; conversions can be easily made (e.g., Beyer and Bommer, 2006, 2007), but this adds uncertainty to the vertical spectrum prediction.

If,in addition to the various criteria discussed thus far in this paper, one were to make it a requirement to predict spectral ratios at response periods below 0.05 s, then only the model of Abrahamson and Silva (1997) would still be in contention. However, that model would not serve for all applications because it does not include an estimate of variability associated with the V/H predictions, and this could only be obtained by calculating all of the residuals for their dataset. Of the 16 studies listed in Table 1, only Campbell and Bozorgnia (2003) performed the exercise

Table 1
Characteristics of GMPEs for Horizontal and Vertical Spectral Accelerations

Study	Data Region	M_{min}	M_{max}	R_{min}	R_{max}	T_{min}	T_{max}
Sabetta and Pugliese (1996)	Italy	4.6	6.8	0	100	0.04	4.0
Ambraseys *et al.* (1996); Ambraseys and Simpson (1996)	Europe and Middle East	4.0	7.5	0	200	0.10	2.0
Abrahamson and Silva (1997)	Western United States/Global	4.4	7.4	0	200	0.01	5.0
Campbell (1997)	Western United States/Global	4.7	8.1	3	60	0.05	4.0
Ambraseys and Douglas (2003)	Global	5.8	7.8	0	15	0.10	2.0
Lussou *et al.* (2001)	Japan	3.5	6.3	10	200	0.02	10.0
Berge-Thierry *et al.* (2003)	Europe and California	4.0	7.9	4	330	0.03	10.0
Campbell and Bozorgnia (2003)	Western United States/Global	4.7	7.7	3	60	0.05	4.0
Kalkan and Gülkan (2004a, 2004b)	Turkey	4.2	7.4	1.2	250	0.10	2.0
Bragato and Slejko (2005)	Northeast Italy	2.5	6.3	0	130	0.10	2.0
Ambraseys *et al.* (2005a, 2005b)	Europe and Middle East	5.0	7.6	0	100	0.05	2.5
Bindi *et al.* (2007)	Northwest Turkey	0.5	5.9	1.5	190	0.10	1.0
Massa *et al.* (2008)	Northern Italy	3.5	6.5	0	100	0.04	2.0
Morasca *et al.* (2008)	Molise, Italy	2.7	5.7	11	39	0.04	2.0
Cauzzi and Faccioli (2008)	Mainly Japan	5.0	7.2	6	150	0.05	20.0
Bindi *et al.* (2010)	Italy	4.0	6.9	1	100	0.03	2.0

of calculating V/H residuals and reporting the standard deviations.

Direct Predictions of V/H Ratios

To our knowledge, there are only four current models for the prediction of V/H ratios as a function of magnitude, distance, and site class. The models of Ambraseys and Simpson (1996) and of Kalkan and Gülkan (2004a) both predict the natural value of the V/H ratio rather than its logarithm, which means that the ratio could become negative for low exceedance levels. There are also other deficiencies with these models, as noted in the discussion in the preceding section (V/H Ratios from Independent Predictions of Spectral Ordinates), but they do not warrant further discussion. The model of Ambraseys and Douglas (2003) is a function only of style of faulting, being based on data from earthquakes of surface-wave magnitude (M_s) 5.8–7.8 and recordings obtained at distances of not more than 15 km from the source. This restriction to very short distances, and the fact that it considers a minimum period of 0.10 s, severely limit the applicability of this model.

The model of Gülerce and Abrahamson (2011) considers the main explanatory variables such as magnitude, distance, and site class in estimating the V/H ratio. Gülerce and Abrahamson (2011) use the horizontal-component Pacific Earthquake Engineering Research–Next Generation Attenuation of Ground Motions (PEER NGA) dataset of Abrahamson and Silva (2008) with small changes due to exclusion of recordings with missing vertical components. The dataset consists of 2,636 recordings from 126 shallow crustal earthquakes from active tectonic regions around the world. The magnitude range of the events is $4.3 \leq M_w \leq 7.9$. The model developers consider both mainshock and aftershock recordings. The rupture distance (closest distance to the rupture plane, R_{rup}) of the records extends as far as 300 km. The proposed model is based on the Abrahamson and Silva (2008) functional form and classifies the sites as a continuous function of V_{S30} (average shear-wave velocity over the top 30 m). The aleatory variability (i.e., sigma) is a function of magnitude, decreasing with increasing magnitude values. The Gülerce and Abrahamson (2011) V/H model accounts for the nonlinear soil response, and this leads to stronger influence of site effects than in most other models, with high V/H ratios on soft soil sites at short distances. The V/H spectral ratio equations are derived for spectral periods up to 10.0 s, based on the recommended usable period ranges of horizontal and vertical ground motions in the PEER NGA database (Chiou *et al.*, 2008).

Database and Record Processing

The V/H model presented here is based on the effort of processing an expanded databank of strong-motion accelerograms from Europe, the Middle East, and the Mediterranean region. These data include the records compiled for the study of Ambraseys *et al.* (2005a), as used by Akkar and Bommer (2007a, 2007b, 2010), from earthquakes of M_w 5 and greater, and the complementary data from smaller events compiled by Bommer *et al.* (2007). The databank has been expanded for all magnitude and distance ranges ($3 < M_w \leq 7.6$ and Joyner–Boore distance $[R_{JB}] \leq 200$ km) by the addition of the new Italian Accelerometric Archive (ITACA) strong-motion database (Luzi *et al.*, 2008) and the recently compiled Turkish strong-motion database (Akkar *et al.*, 2010). Accelerograms with $M_w \geq 4.5$ and $R_{JB} \leq 100$ km are selected from this databank for the derivation of the V/H model. Figure 2 presents the M_w–R_{JB} distribution of the 1267 accelerograms used in this study in terms of style of faulting and site class. The accelerograms were recorded from a total of 392 earthquakes that occurred in Europe and the surrounding regions. The style of faulting (SoF) is deter-

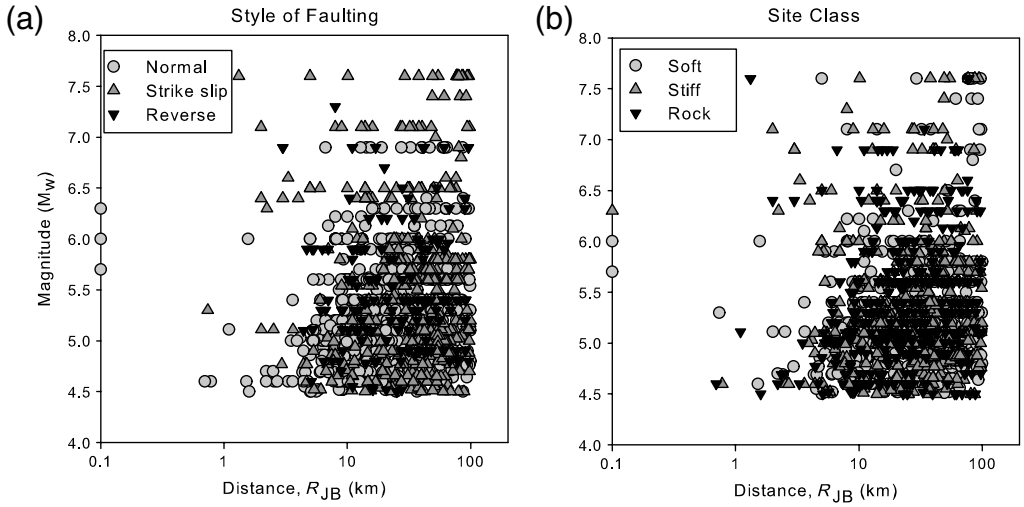

Figure 2. Magnitude vs. distance distribution of records used in the V/H model in terms of (a) style of faulting and (b) site class.

mined by using (a) the P, T, and B parameters of the fault plane solutions (Frohlich and Apperson, 1992) whenever they are available and (b) the rake angle intervals proposed by Boore *et al.* (1997), Campbell (1997), and Sadigh *et al.* (1997). This approach used for classifying the style of faulting has been the state of practice in the previously compiled European datasets; we chose not to update it by following the recent NGA criteria, which differ from one model developer to another (Abrahamson *et al.*, 2008). The site classification is based on specific V_{S30} intervals, inferred either from *in situ* geophysical measurements or geological explorations, and it is consistent with the site-class definitions described in EC8 (Eurocode 8, 2004) and NEHRP (2009): rock ($V_{S30} \geq$ 750 m/s), stiff soil (360 m/s $\leq V_{S30} <$ 750 m/s), and soft soil (180 m/s $\leq V_{S30} <$ 360 m/s). Major features of earthquakes in the database, number of accelerograms used from each event, and their distance ranges are given in Table A1 (see Appendix).

The long-period filter parameters (low-cut filter values) are determined by applying the criteria outlined in Akkar and Bommer (2006). For the selection of high-cut filter values, the high-frequency noise behavior discussed in Douglas and Boore (2011) is used. After identifying the noisy portion at the high-frequency end of the Fourier acceleration spectrum, it is removed by choosing a high-cut filter value that is judged to be appropriate. On the basis of the results in Akkar *et al.* (2011), the high-cut filtering influence becomes negligible for vibration periods greater than 0.05 s. The current database consists of horizontal and vertical accelerograms for which the spectral ordinate of the filtered record differs by less than 10% from that of the mean-removed record for $T \leq 0.05$ s. This criterion was proposed by Akkar *et al.* (2011) after looking at the simple statistics of the spectral ratios of the filtered to mean-removed records at several short-response periods for both the horizontal and vertical components. For periods longer than 0.05 s, the criteria described in Akkar and Bommer (2006) are applied to minimize the filtering distortions at longer periods. Figure 3 shows the period-dependent data variation in terms of SoF and site class after applying the Akkar and Bommer (2006) and Akkar *et al.* (2011) criteria. Regardless of SoF and site classes, the loss of data due to filtering effects becomes noticeable after $T = 1.0$ s. There is also a significant loss of events with multiple recordings at $T = 3.0$ s that results in an increase in the percentage of singly-recorded earthquakes in the database. On the basis of these observations, it was judged that at periods beyond 3.0 s the data would be insufficient to allow robust regression analyses, and this was therefore selected as the limiting period for the proposed V/H model in this study.

Regression Analyses

The actual V/H trends at several vibration periods and several functional forms (complex to simple) are explored before executing the final regression analyses. This section first describes the behavior of V/H trends under different estimator parameters and then presents our observations on different functional forms that identified the optimum V/H model proposed in this study.

Observed Trends of V/H Ratios with Explanatory Variables

Figure 4 shows the average V/H ratios for a set of predetermined spectral periods ($T = 0.0$ [PGA], 0.10, 0.20, 0.40, 1.0, and 2.0 s). For a given period, the data are divided into three magnitude ranges (i.e., $4.5 \leq M_w < 5.5$, $5.5 \leq M_w < 6.5$, and $M_w \geq 6.5$) and the data falling into these M_w intervals are clustered into 10-km distance bins. The data are initially modified for strike-slip faulting and rock site conditions by using empirical scaling factors obtained from a preliminary set of regression analyses in order to utilize the

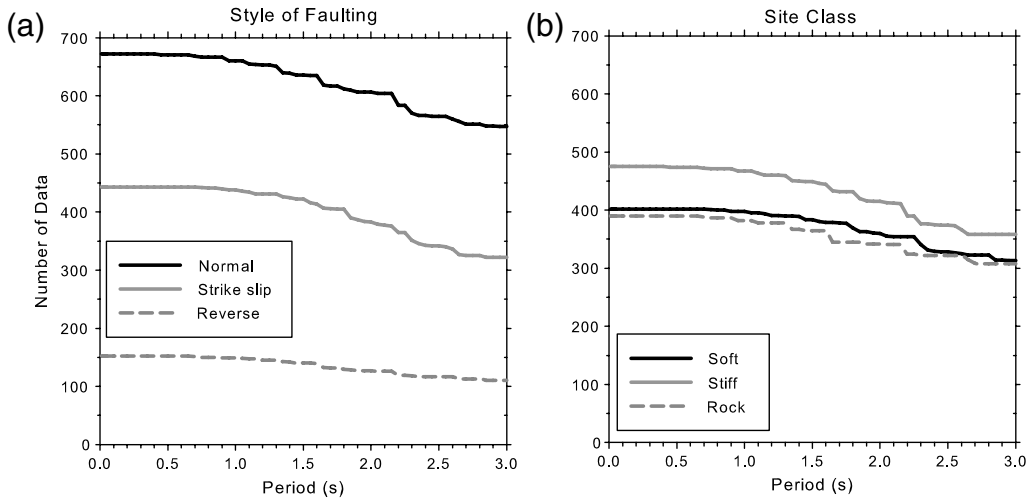

Figure 3. Period-dependent variation of usable recordings as a function of (a) style of faulting and (b) site class.

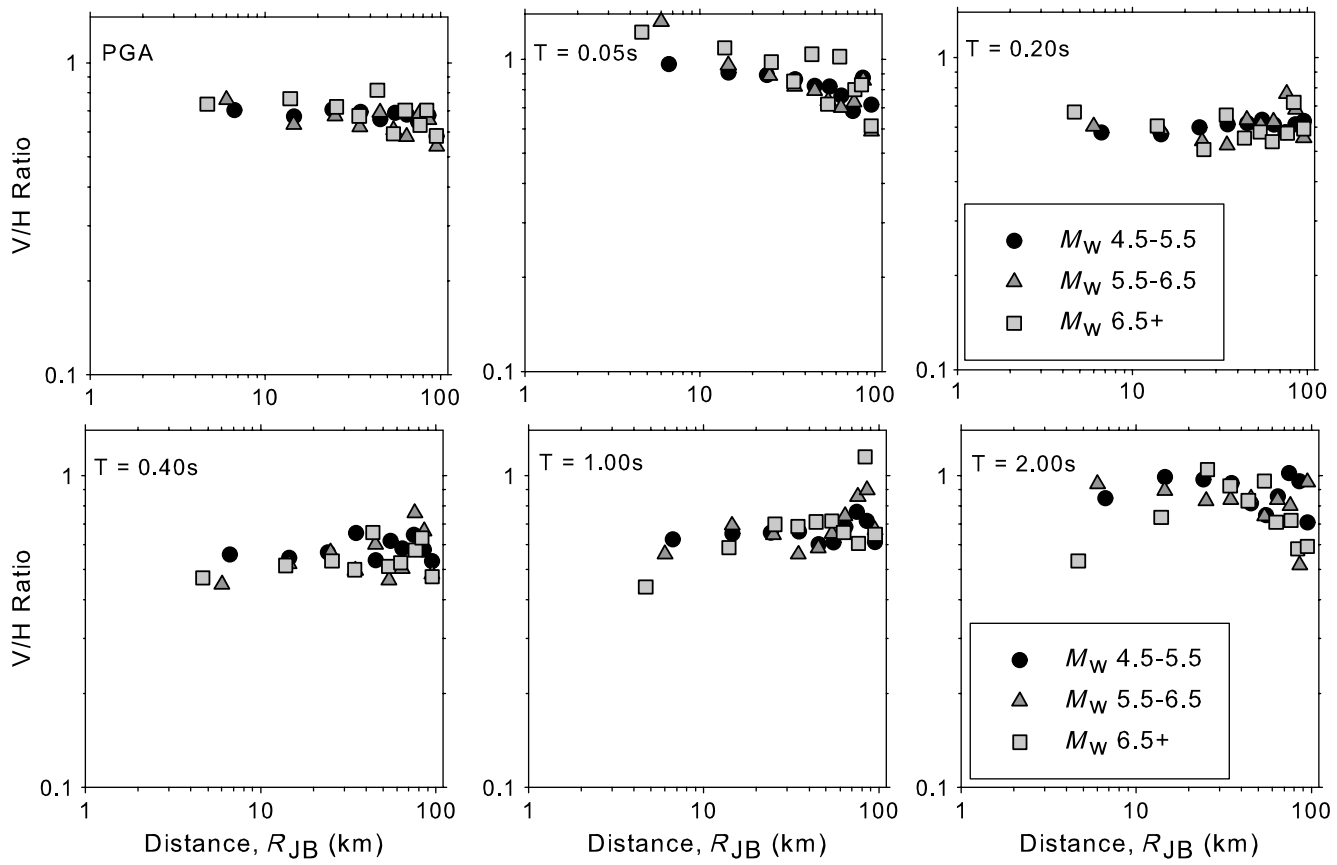

Figure 4. Average V/H ratios as a function of distance for a set of spectral periods for three magnitude intervals: $4.5 \leq M_w < 5.5$, $5.5 \leq M_w < 6.5$, and $M_w \geq 6.5$. The average V/H ratios are calculated for distance bins of 10 km. The data are initially modified for strike-slip and rock site conditions by using empirical scaling factors obtained from a preliminary set of regression analyses.

results of the whole dataset in the examination of V/H trends. The average V/H ratio of each distance cluster is plotted on the scatter diagram of the corresponding spectral period. The average V/H ratio is computed whenever the number of records in a cluster is greater than 4. Regardless of the spectral period, the V/H trends in Figure 4 do not display strong magnitude dependence. The data from the largest magnitude interval (i.e., $M_w \geq 6.5$) also do not exhibit a significant saturation trend at short periods and at close distances. The ratios tend to decay with increasing distance for $T \leq 0.05$ s, they are almost independent of distance at $T = 0.20$ s, and they mildly increase with increasing distance for $T \geq 0.40$ s. The gradient of distance-dependent V/H variation seems to be free of magnitude effects. Several investigators offered seismological explanations for the observed dependency of V/H on distance that are related to *S*-to-*P*-wave conversion and the dominance of incident *SV* and *P* waves, depending on the source-to-site distance and other geological conditions (Kawase and Aki, 1990; Silva, 1997; Amirbekian and Bolt, 1998; Beresnev *et al.*, 2002). These discussions are beyond the scope of this study, and the interested reader is referred to the literature cited previously in this paper for further information. The V/H becomes maximum at very short periods and attains minimum values at $T = 0.20$ s and $T = 0.40$ s.

Exploration of Functional Forms

Three functional forms are investigated in the light of observations presented in the previous section. The base functional form is presented in equation (1), which considers magnitude-dependent geometrical spreading and also includes a second-order magnitude term to account for the saturation effects. This functional form has been used in Akkar and Bommer (2007a, 2007b, 2010) and Bommer *et al.* (2007) to estimate PGA, peak ground velocity (PGV), and 5%-damped spectral ordinates for the previous versions of the pan-European strong-motion databases:

$$\log_{10}(Y) = b_1 + b_2 M_w + b_3 M_w^2 + (b_4 + b_5 M_w) \log_{10} \sqrt{R_{JB}^2 + b_6^2} + b_7 S_S + b_8 S_A + b_9 F_N + b_{10} F_R. \quad (1)$$

In equation (1), S_S and S_A are dummy variables taking the value of 1 for soft (180 m/s $\leq V_{S30} <$ 360 m/s) and stiff

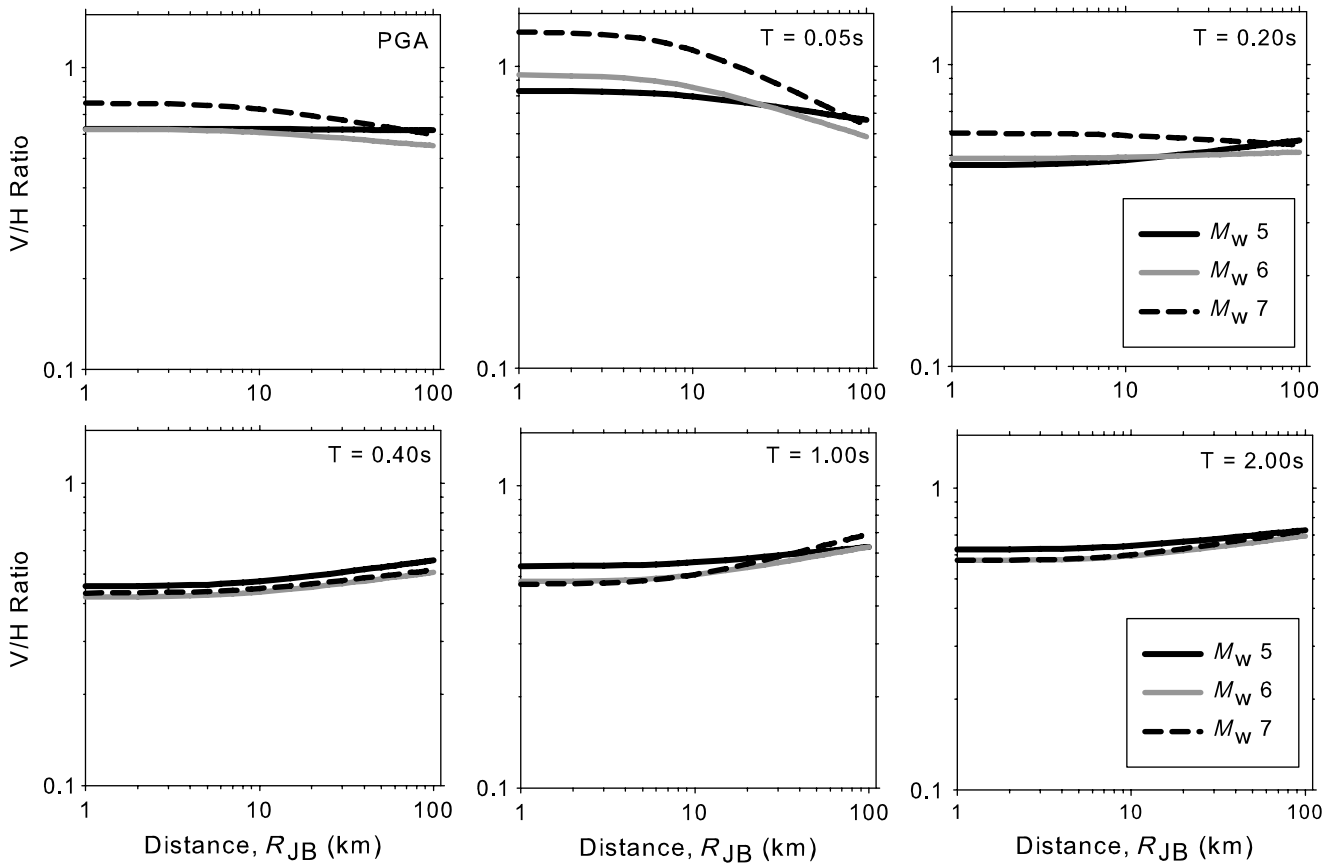

Figure 5. Median V/H trends for a set of spectral periods as a function of magnitude and distance using equation (1).

(360 m/s $\leq V_{S30} <$ 750 m/s) sites, respectively (and 0 otherwise), and F_N and F_R are similarly defined for normal and reverse faulting earthquakes, respectively. The hypothetical depth term b_6 is kept as 7.5 km while exploring the functional forms.

Figure 5 presents the median V/H trends obtained by running the regression analysis for equation (1). The regression analysis is conducted using the one-stage maximum-likelihood technique proposed in Joyner and Boore (1993). The plots use the same set of spectral periods given in Figure 4 and show the variation in median V/H as a function of distance for M_w 5, 6, and 7 (midpoints of magnitude clusters used for the discussion of actual data trends in Figure 4). The median curves in Figure 5 display a significant sensitivity to the changes in magnitude at short periods. For PGA, the median V/H curve of M_w 5 is between the corresponding curves of M_w 6 and 7, for which it would be difficult to provide a physical explanation. As for the longer-period (i.e., $T \geq 0.4$ s) median V/H behavior, the ambiguity in terms of magnitude scaling still persists. This time the median V/H curves of M_w 7 almost overlap the M_w 6 median curves. These observations are contrary to the actual data trends discussed in the previous section, and they suggest not using equation (1) for estimating the V/H ratio. It may also be the case that the database used in this study may not be sufficient to fully constrain the complex seismological estimator terms in equation (1). On the basis of the preceding discussions, two simplified versions of equation (1) are evaluated to determine the most appropriate functional form for the proposed V/H model. The first simplified version mutes the coefficient b_5 (magnitude-dependent multiplier on the distance term), and the second version (the simplest among all tested functional forms) mutes both b_3 (second-order magnitude term that accounts for saturation effects) and b_5. Median V/H ratios are presented in Figure 6 for the second simplified version. In view of the median curves presented in Figure 6, the simplest functional form seems to fit very well the V/H trends of the actual data. This form avoids the deficiencies discussed for equation (1) and yields unbiased estimations that are verified by conventional residual analysis, which is described in detail in the next section.

Regression Analyses

Regression analyses to estimate V/H ratios for PGA and 5%-damped spectral accelerations up to a period of 3.0 s are conducted for the simplest functional form that is found to be optimal with respect to the other two alternatives. We do not

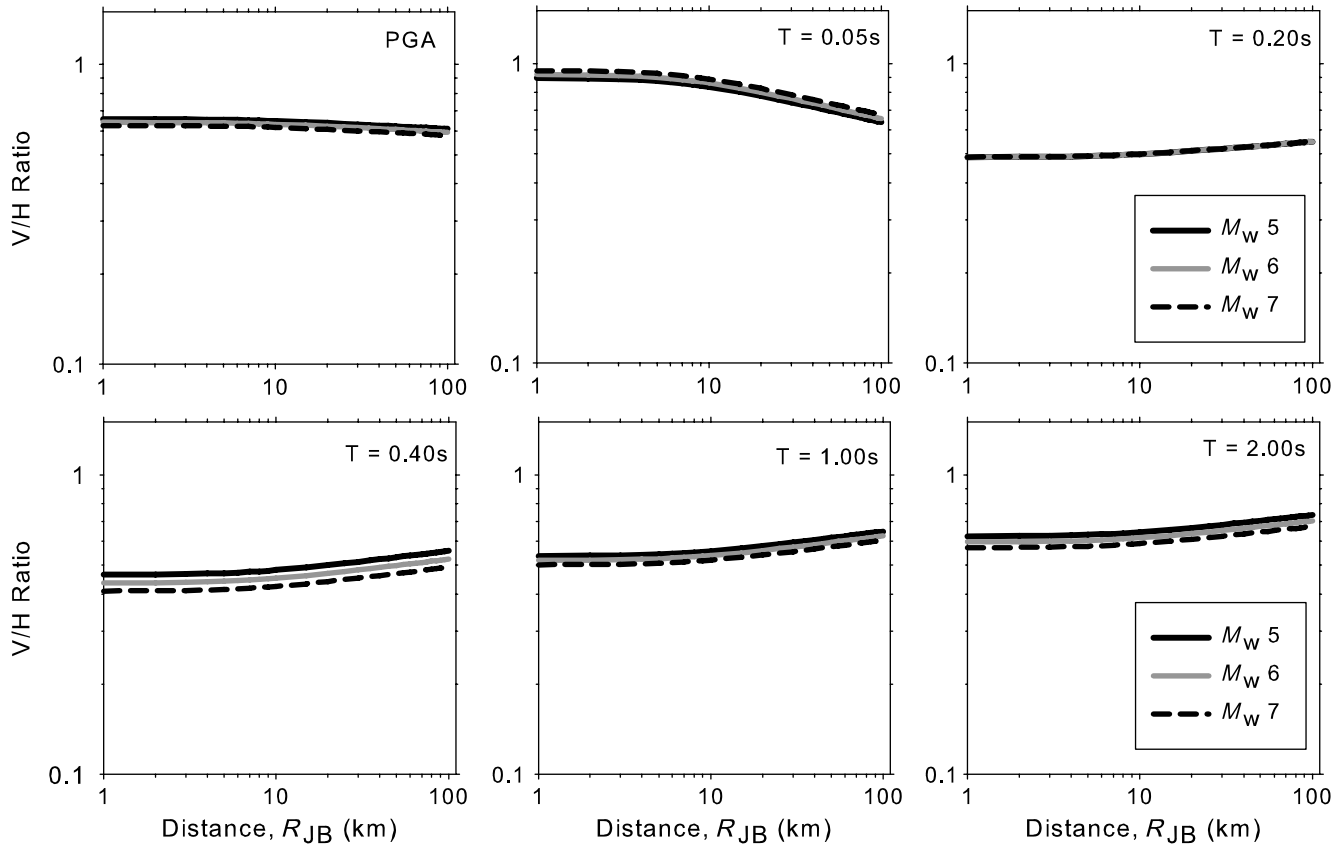

Figure 6. Median V/H trends for a set of spectral periods as a function of magnitude and distance using equation (1) with $b_3 = b_5 = 0$.

derive V/H ratios for PGV because vertical PGV is not widely used in current engineering design practice. The aleatory variability is represented by homoscedastic sigma, as in the case of Akkar and Bommer (2010), and it is decomposed into inter- and intraevent components. The final functional form is given in equation (2) for completeness:

$$\log_{10}(V/H) = b_1 + b_2 M_w + b_4 \log_{10}\sqrt{R_{JB}^2 + b_6^2} + b_7 S_S + b_8 S_A + b_9 F_N + b_{10} F_R. \quad (2)$$

Table A2 (see Appendix) presents the regression coefficients of the proposed V/H model. The hypothetical depth coefficient (b_6) is set at 5 km in the final computations because this value resulted in a slightly narrower distribution of residuals. The last three columns in Table A2 list the intraevent (σ_{intra}), interevent (σ_{inter}), and total (σ_{total}) standard deviations of the model. The period-dependent variations of standard deviations are also given in Figure 7; it shows that, independent of period, the total standard deviation is approximately 0.2. The level of total sigma computed in this study is similar to those presented in the recent V/H models (e.g., Gülerce and Abrahamson, 2011; Bozorgnia and Campbell, 2004b); this is explored further in the following sections. Interevent variability is the minor contributor to the total standard deviation, as is generally the case for empirical GMPEs. The minor role of this component on the variability is, as expected, even smaller for the V/H ratios because the

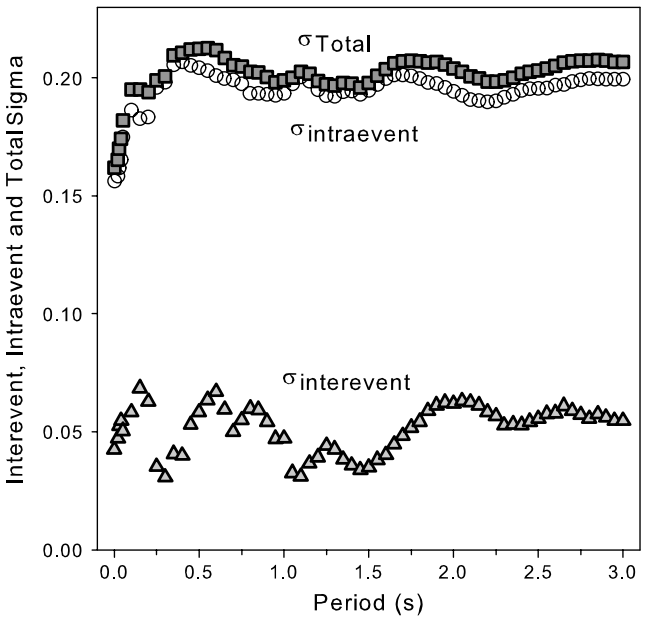

Figure 7. Period-dependent variations of standard deviations of the proposed V/H GMPEs.

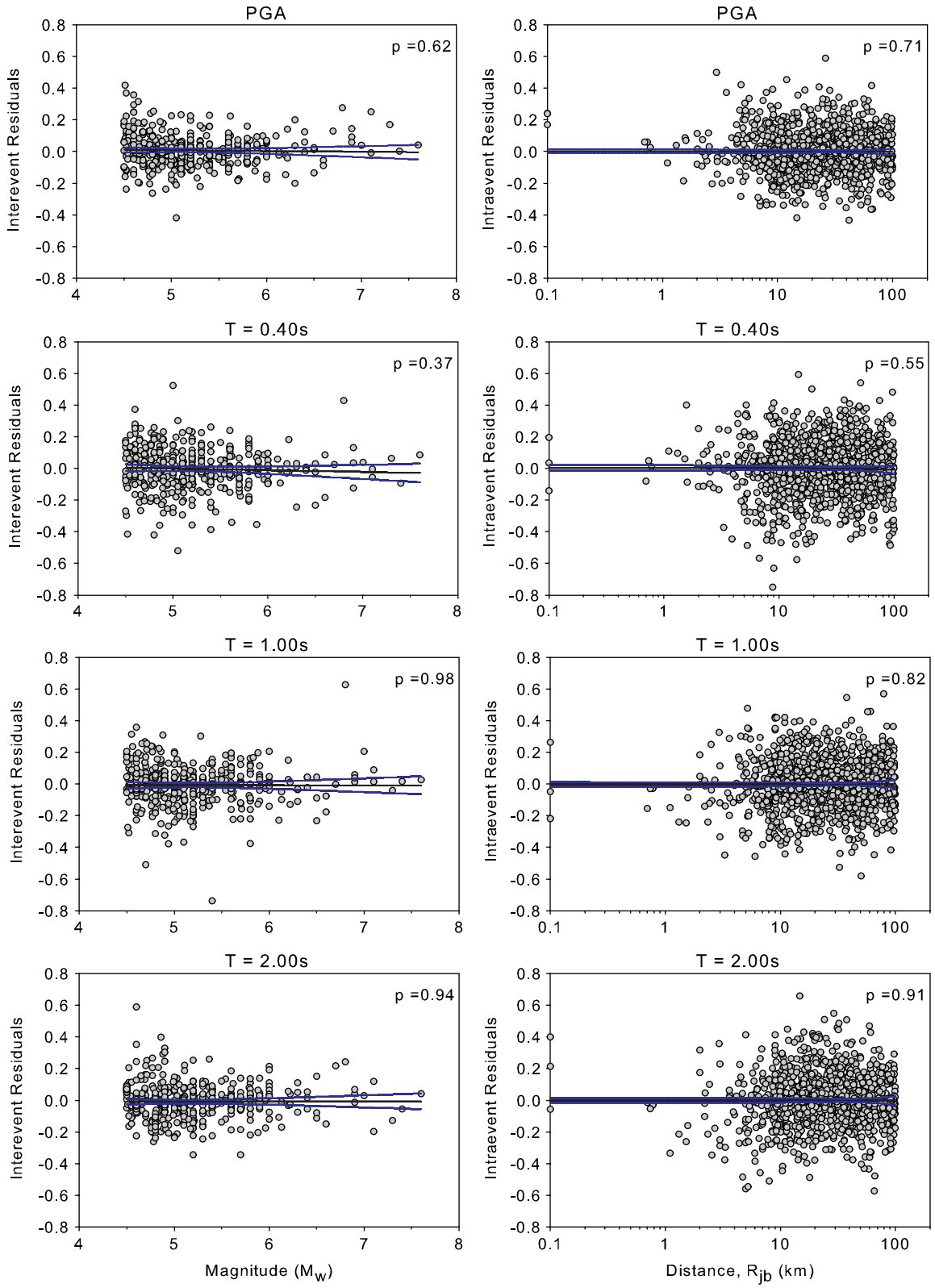

Figure 8. Inter- and intraevent residual scatters of V/H estimations for four spectral ordinates: PGA and $T = 0.4$, 1.0, and 2.0 s. The color version of this figure is available only in the electronic edition.

interevent terms of vertical and horizontal ground-motion components (which are correlated) cancel each other, which results in an overall reduction in the interevent variability of the proposed model.

The overall performance of the proposed V/H GMPEs is evaluated through conventional residual analysis. Figure 8 shows the inter- and intraevent residual scatters of preselected short- to long-period V/H estimates (i.e., PGA and $T = 0.4$, 1.0, and 2.0 s). The possible bias in median V/H estimates with respect to magnitude is investigated by studying the interevent residual trends (left panel in each row). The dependence of median V/H estimates on distance is explored from the intraevent residuals (right panel in each row). The plots also contain straight-line fits and their 95% confidence intervals to better visualize the possible trends in residuals in terms of these estimator parameters. Whenever the straight-line fits have a slope term that is significantly different than zero, the V/H estimates can be considered as biased for the corresponding estimator parameter.

We applied sample t statistics to test the null hypothesis that the slope term of a straight-line fit is zero. The significance level (p) provided by this statistical test is used for rejecting or not rejecting the null hypothesis. A p value that is well above 0.05 is generally accepted as sufficient for not rejecting the null hypothesis, namely the insignificance of the slope term in the straight-line fit. The results in Figure 8 indicate a fairly good performance in the median V/H estimates from the model proposed in this study. The p values presented in the upper right corners of the magnitude- and distance-dependent residual plots attain values much larger than 0.05. This observation suggests that the slopes of the straight-line fits are not significant and that there is no model misfit for magnitude and distance. Relatively large residuals at the high- and low-magnitude ranges can result from the uneven data distribution toward larger magnitudes and increased magnitude uncertainty for smaller events. Nonetheless, the overall evaluations suggest an acceptable level of accuracy in the V/H estimates of the proposed model.

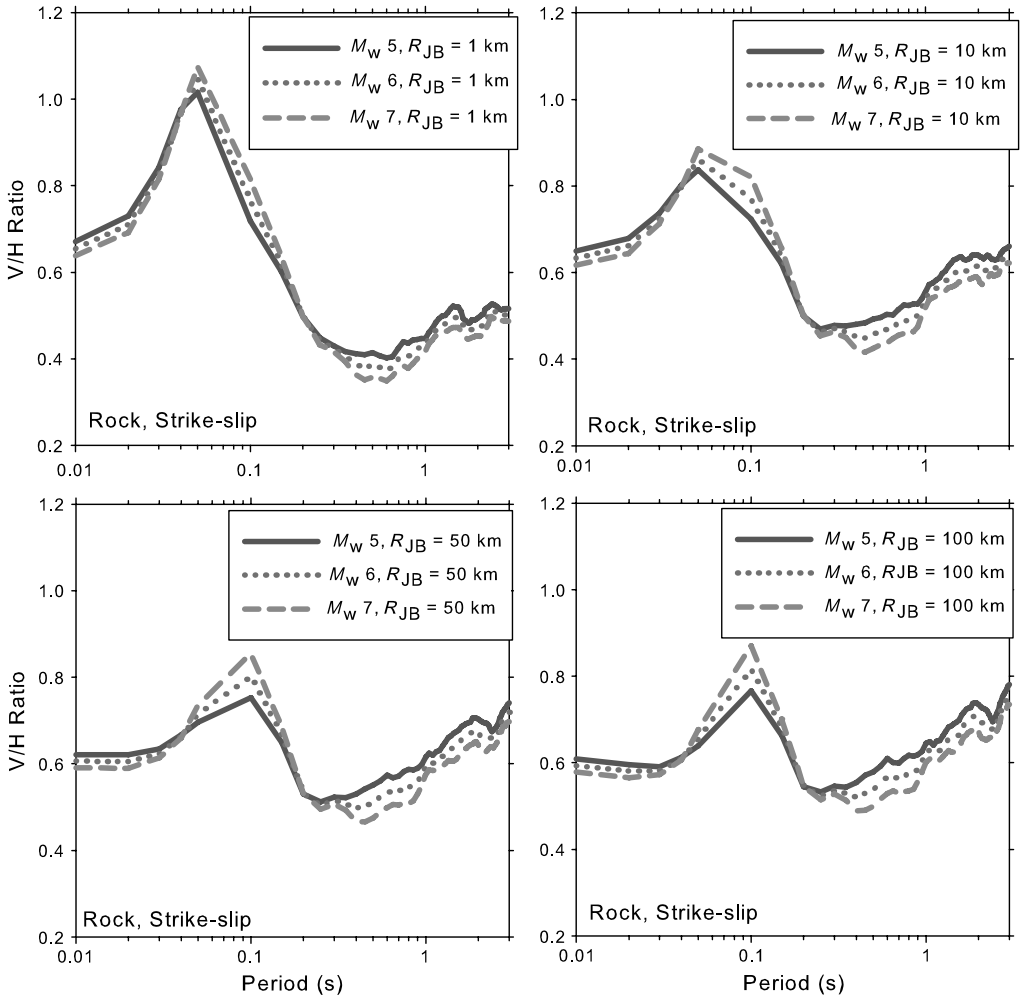

Figure 9. Median V/H spectra for different magnitude and distance ranges computed from the proposed model.

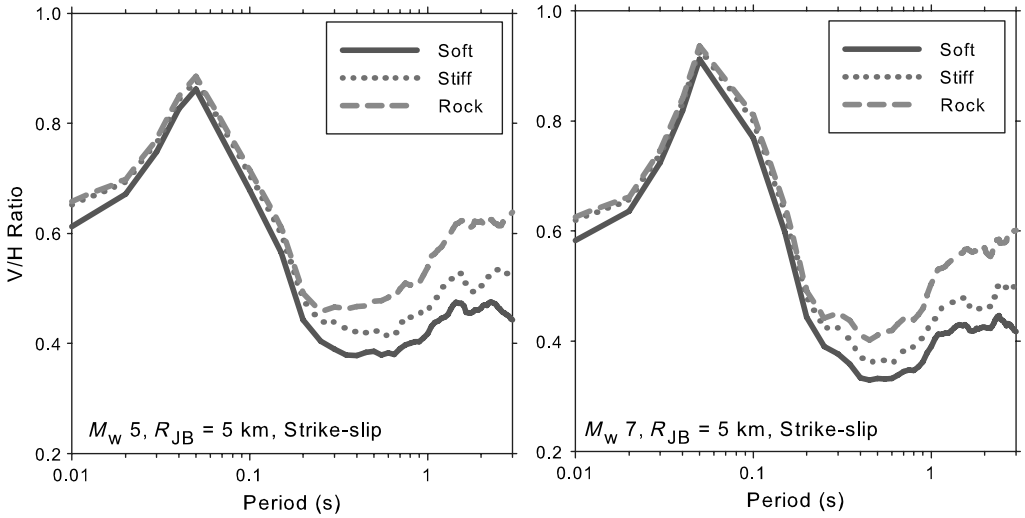

Figure 10. Median V/H spectra for different site classes for a site located at a distance of $R_{JB} = 5$ km from a strike-slip fault.

Predicted V/H Spectral Ratios

Variations in median V/H under the influence of the considered explanatory variables are presented in this section through different scenarios. We also compared the estimations of our model with the recent V/H GMPEs of Gülerce and Abrahamson (2011) and Bozorgnia and Campbell (2004b) (abbreviated as GA11 and BC04, respectively). These models constitute the most up-to-date developments on V/H ratio predictions and provide sigma values that are a fundamental requirement for this application.

Median V/H Ratios of the Proposed Model and Associated Variability

Figure 9 shows the variation of median V/H spectra for the entire period band by considering the specific magnitude and distance combinations for strike-slip faulting and rock site conditions. V/H ratios corresponding to PGA are presented at $T = 0.01$ s in Figure 9, as well as in Figures 10 to 15, because PGA mimics the spectral acceleration at $T = 0.01$ s. The plots confirm the negligible effect of magnitude on V/H ratios. Small magnitude events result in slightly larger V/H ratios at very short periods (i.e., $T \leq 0.04$ s) and for $T > 0.2$ s. This trend is reversed between these two response periods. The V/H ratio attains its maximum at very short periods that increase slightly with increasing distance. Independent of the variations in magnitude and distance, the V/H spectrum tends to increase for $T \geq 0.5$ s. This trend is more noticeable at larger distances.

Figures 10 and 11 show the median V/H estimations for different site classes and style of faulting, respectively. Both figures consider a site located 5 km from the causative

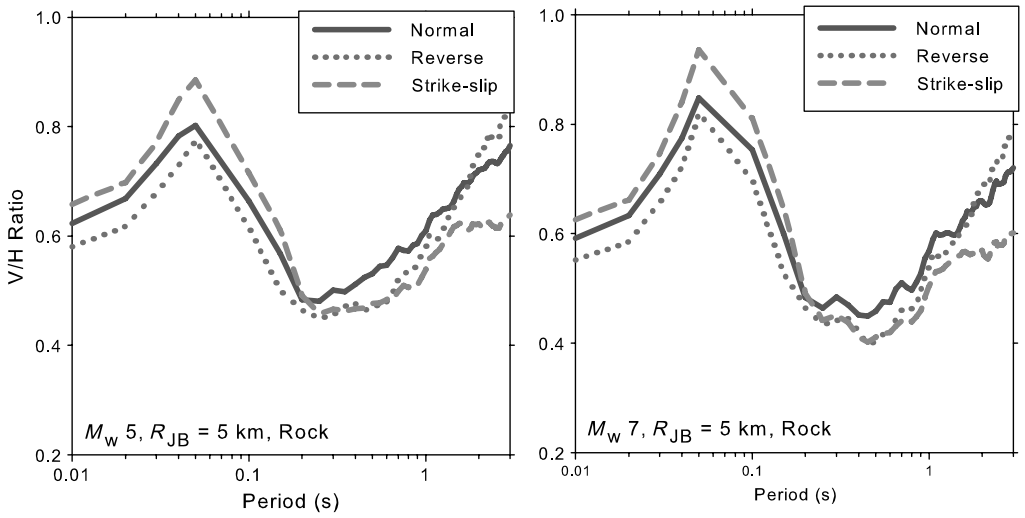

Figure 11. Median V/H spectra for different style of faulting for a rock site located $R_{JB} = 5$ km from the causative source.

fault rupture of small and large magnitude earthquakes with M_w 5 and 7, respectively. The V/H spectra in Figure 10 indicate that the site term becomes influential for $T > 0.20$ s, and it is independent of the variations in magnitude. The difference between the V/H ratios steadily increases with the stiffness of the site, and it becomes more apparent towards longer periods. The V/H plots in Figure 11 show the dominance of strike-slip events in the short-period interval with respect to the other style of faulting. The median V/H values resulting from normal and reverse events exceed the strike-slip V/H ratios as the period shifts toward the long-period range of the spectrum. These patterns are consistent with the predictive V/H models proposed by Bozorgnia and Campbell (2004b) and Gülerce and Abrahamson (2011). The latter models also suggest the dominance of strike-slip V/H ratios in the short periods that are overtaken by either normal or reverse style of faulting in the longer period range.

The final plot (Fig. 12) in this section compares the median and eighty-fourth percentile V/H spectra for different magnitude levels (M_w 5, 6, and 7). The earthquake scenario used in the comparisons is a rock site located at a Joyner–Boore distance of 5 km from a strike-slip event. The comparative plots indicate that the eighty-fourth percentile V/H spectra range is between 1.0–1.4 at short periods and that they are bounded between 0.8–1.0 for longer periods. These values are approximately 60% larger than the median V/H spectra and can be considered as valid for the entire magnitude and distance range of the model.

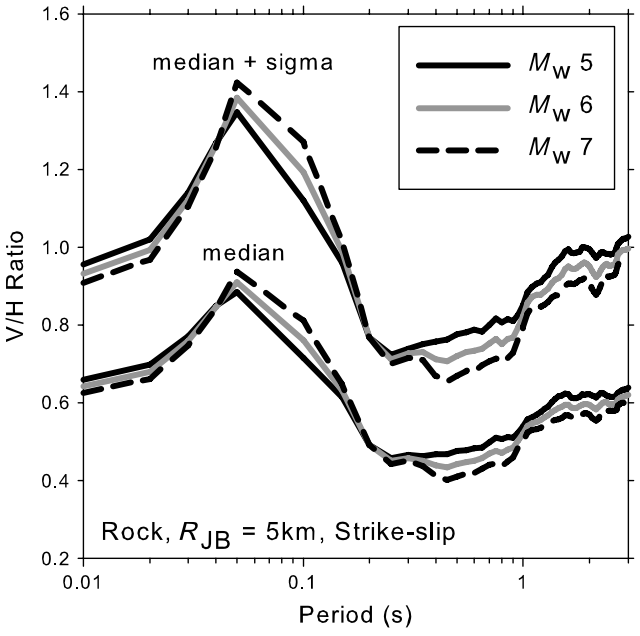

Figure 12. Median and 84-percentile V/H spectra for different magnitude levels for a rock site located at $R_{JB} = 5$ km from a strike-slip fault.

Comparisons with Other Studies

The models compared herein all use M_w. GA11 uses R_{rup} for the distance term. The distance metric in BC04 is R_{SEIS} (shortest distance to the assumed zone of seismogenic rupture on the fault), and the proposed model describes source-to-site distance by R_{JB}. All of these distance metrics depend on the fault geometry, depth to top of rupture, and rupture dimension that are associated with the event size and style of faulting. The particular features controlling each distance metric are accounted for by using empirical relationships proposed in the literature (Scherbaum *et al.*, 2004). The magnitude-dependent depth-to-top-of rupture (Z_{TOR}) values proposed by Abrahamson *et al.* (2008), seismogenic depth (d_{seis}) information given in Campbell (1997), and rupture dimension relationships in Wells and Coppersmith (1994) are used for calculating the distance metrics of concern for a vertical strike-slip fault. The R_{JB} and R_{SEIS} distances are calculated for the magnitude scenarios of M_w 5, 6, and 7 by setting R_{rup} equal to 10 km. For M_w 5, 6, and 7, d_{seis} takes the values of 7.1, 4.9, and 3 km, respectively (Campbell, 1997). Accordingly, R_{seis} equals 10.7, 10.57, and 10.4 km for M_w 5, 6, and 7, respectively. The R_{JB} values are calculated as 8, 9.37, and 9.95 km for M_w 5, 6, and 7, respectively, when the corresponding magnitude-dependent Z_{TOR} values are estimated as 6, 3.5, and 1 km from Abrahamson *et al.* (2008). The chosen magnitudes, as well as the distance, are covered by all the GMPEs considered in the comparisons. The comparisons are based on a generic rock site and a generic soil site. The former site is described by a V_{S30} of 620 m/s, whereas the latter is suggested to have a V_{S30} value of 310 m/s (Bozorgnia and Campbell, 2004b); the same shear-wave velocities are used in GA11. The generic rock site is mimicked by the geometric mean of rock and stiff sites for our model (notwithstanding the appreciable uncertainty in site classification of European strong-motion stations). We assumed that the soft-soil description of our model can represent the generic soil condition in the comparisons.

Figure 13 presents the comparisons for the specific scenarios described in the preceding paragraph. The upper two rows show the comparisons for a generic rock site, whereas the lower two plots compare the models for generic soil condition. The first row in each pair shows the comparisons for median V/H spectra, whereas the plots under the median V/H estimations display the same information for the eighty-fourth percentile spectra. The first column of plots in this figure compares the GMPEs for a scenario earthquake of M_w 5. This is followed by M_w 6 and M_w 7 cases in the second and third columns, respectively. Models are plotted for the spectral period ranges suggested by the authors of the models. The immediate observation from the comparative plots is the consistent V/H trends among all GMPEs. For generic rock comparisons, the median V/H spectra of GA11 and this study follow each other closely except for

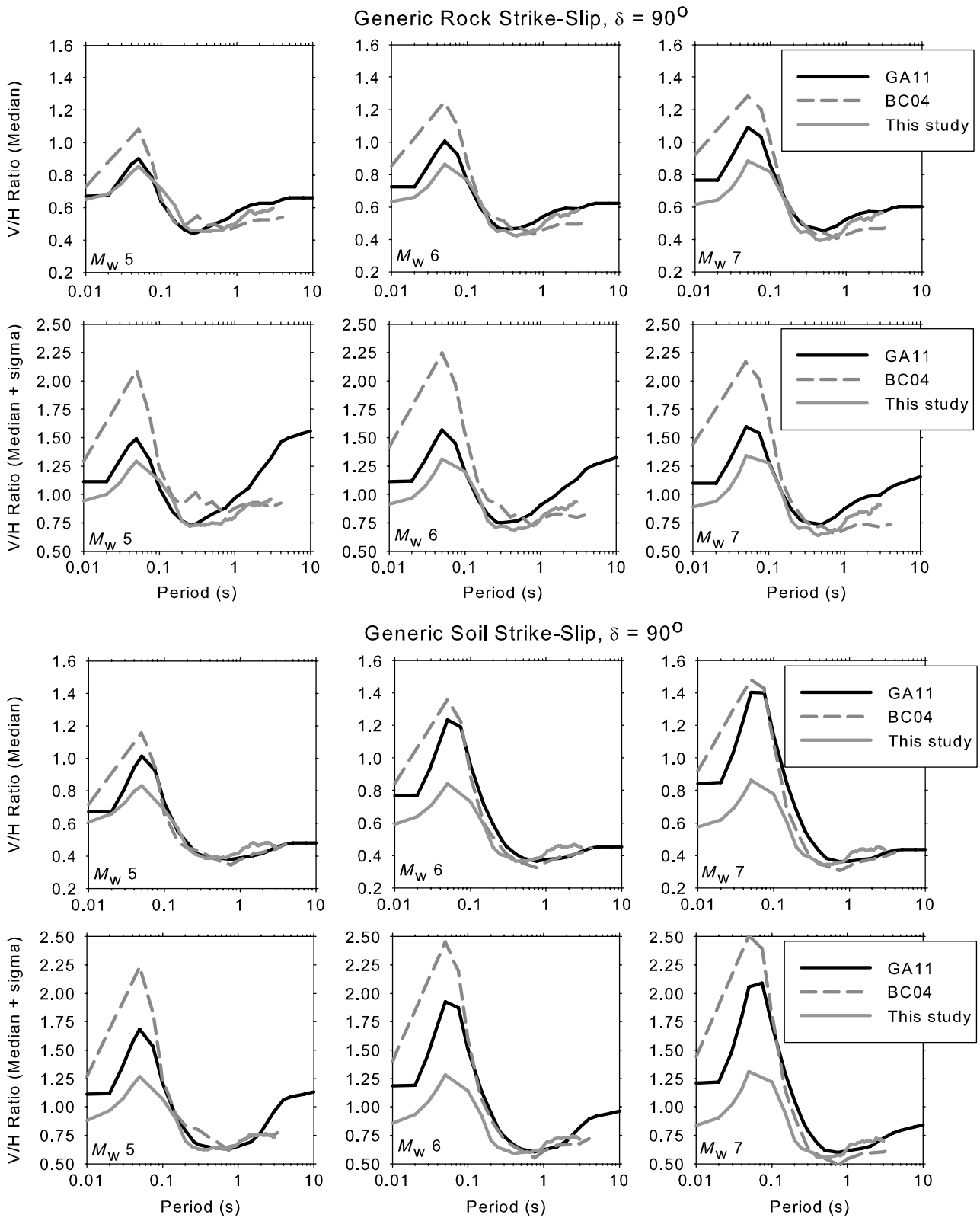

Figure 13. Comparisons of selected V/H GMPEs with the proposed model at different magnitudes for a generic rock site (upper 2 rows) and generic soil site (lower 2 rows) located at a distance of $R_{rup} = 10$ km from a vertical strike-slip fault (*i.e.*, dip angle, $\delta = 90°$). The selected models are abbreviated with the initials of their developers: GA11 stands for Gülerce and Abrahamson (2011) and BC04 is Bozorgnia and Campbell (2004b).

the short-period V/H values of the M_w 7 case, where GA11 yields higher estimations. The discrepancy between our model and that in GA11 increases with increasing magnitude for the median estimations of generic soil class. Speculatively, this can be attributed to the lack of soil nonlinearity in our model, as well as to the uncertainty imposed by the generic site class definitions in our database. Regardless of the magnitude, the discrepancy between these models increase for the eighty-fourth percentile spectra as GA11 estimations are considerably higher than this study. The BC04 model generally agrees well with this study and GA11 for $T > 0.1$ s, independent of the variations in magnitude, site, and exceedance level. The BC04 model estimates rather high V/H ratios at short periods with respect to GA11 and this study for rock sites. Both GA11 and BC04 predict similar median V/H estimations for the generic soil at short periods, but this consistent trend diminishes for the eighty-fourth percentile spectra, as BC04 estimates are higher with respect to GA11. We believe that any apparent regional differences at the larger magnitudes that drive seismic hazard assessments arise predominantly from data distributions and functional forms rather than pronounced and systematic regional differences. Having said this, the presented model as well as the other ones discussed in the paper, are applicable to active regions of shallow crustal seismicity, and additional work would be required before applying them to subduction zones or stable continental regions. Figure 14 compares the total sigma values (transformed to natural logarithms) from these three models, all of which are heteroscedastic except for the new model derived in this study. As can be immediately appreciated from this figure the aleatory variability of the current model is generally rather low compared with the others. For the M_w 7.5 case, the Bozorgnia and Campbell (2004b) model has slightly smaller sigma values at longer periods with respect to the new model.

The last set of comparisons presented in this section comprise the V/H ratios obtained from our model and those of Ambraseys *et al.* (2005a, 2005b) that estimate the horizontal and vertical spectral ordinates from separate expressions. The Ambraseys *et al.* model was derived using a different dataset for estimating the ground motions for Europe and the Middle East. Because it estimates the maximum of two horizontal components, we used the empirical adjustment factors in Beyer and Bommer (2006, 2007) to convert their horizontal spectral estimates to a geometric-mean horizontal-component definition. No further adjustment is required between the two models because they use the same estimator parameters for magnitude and distance. Both models use the same methodology for site classification. The comparisons are done only for the rock site scenario that is described in the previous paragraphs and are presented in Figure 15. The models agree fairly well for M_w 6 but differ for the smaller (M_w 5) and larger (M_w 7) events. The observed differences at large and small magnitudes tend to diminish with increasing period (i.e., $T > 0.2$ s). The V/H ratios calculated from Ambraseys *et al.* (2005a, 2005b) are sensitive to the magnitude variations, which is observed neither in our model nor in the models discussed in the previous paragraphs. The pronounced differences between these two pan-European models may stem from the database differences. The database presented in this study is larger than the Ambraseys *et al.* database; it also contains more up-to-date metadata information, particularly for the site classes of strong-motion stations. Another source of difference between these models could be the discrepancy in the lower magnitude limits because Ambraseys *et al.* (2005a, 2005b) considers events with $M_w \geq 5$, whereas the smallest magnitude in our model is M_w 4.5. Differences in the magnitude ranges of predictive models may seriously affect their ground-motion estimations (Bommer *et al.*, 2007).

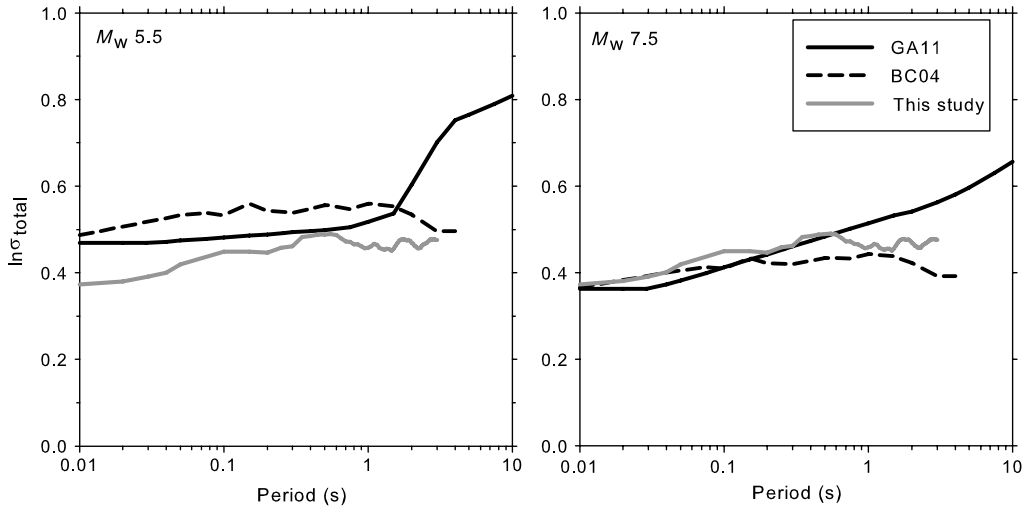

Figure 14. Total sigmas of ln(V/H) for spectral ordinates as a function of response period for the four models and for small (*left*) and large (*right*) magnitudes.

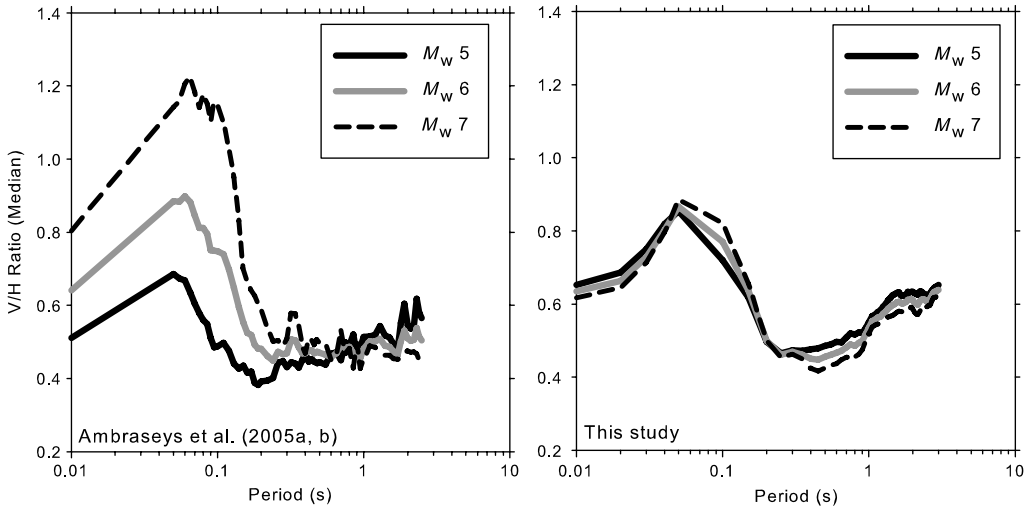

Figure 15. Comparisons of median V/H ratios between Ambraseys *et al.* (2005a, b) (*left*) and this study (*right*) for the same scenario described in Figure 13.

Discussion and Conclusions

In this paper we have presented a model for the prediction of the ratios of vertical-to-horizontal spectral accelerations at response periods up to 3.0 s, using strong-motion data from Europe and the Middle East. We believe that the model can be used to estimate the distribution of V/H ratios of ground motions generated by shallow crustal earthquakes in this region with magnitudes from M_w 4.5 to 7.6. The equations predict V/H ratios as a function of magnitude, style of faulting (reverse, normal, strike-slip), distance, and site classification (rock, stiff soil, soft soil). The equations are applicable for Joyner–Boore distances up to 100 km, which is likely to be sufficient because V/H ratios will generally be applied to scenarios determined from disaggregation of PSHA. For regions of crustal seismicity and for annual exceedance frequencies of engineering interest, the controlling earthquake scenarios will usually be located at relatively short source-to-site distances. The model uses a rather simple functional form, and its extrapolation for magnitudes and distances exceeding the bounds of the dataset should be performed with caution.

This new V/H model addresses a lack of predictive equations for the logarithm of vertical-to-horizontal ratios of response spectral ordinates as a function of these explanatory variables, and it is the first such model derived specifically for application in the European, Mediterranean, and Middle Eastern regions. In order to fully address the issue of epistemic uncertainty in ground-motion prediction, a single predictive model is not sufficient. Having said this, fewer models are required for V/H ratios than those included in the logic-tree formulation for the horizontal response spectra (e.g., Bommer *et al.*, 2005) because the epistemic uncertainty in the ground motion will already be captured to a large degree in the horizontal motion. Nonetheless, a comprehensive PSHA should also address the epistemic uncertainty in the prediction of the V/H ratios. A feasible approach would be to combine this new model with that of Gülerce and Abrahamson (2011), which is derived from the NGA dataset and, if a third model is required, that of Bozorgnia and Campbell (2004b), notwithstanding that the latter does not cover the shortest response periods. Because it has been shown that the NGA models are applicable to the European region (Stafford *et al.*, 2008), combining the Gülerce and Abrahamson (2011) model with the model presented in this paper may offer a suitable way to capture epistemic uncertainty in V/H ratios for seismic hazard analyses in Europe. We might also dare to suggest that pending the publication of new V/H models from the NGA-West 2 project (see Data and Resources), the same combination of V/H models could be used meanwhile in hazard studies in western North America. The two models—Gülerce and Abrahamson (2011) and our European model—are compatible, or at least consistent, in terms of parameter definitions, a fact that facilitates their combination. One exception to this is that, whereas their model employs the R_{rup} distance metric, we use R_{JB}; this means that adjustments will be needed (Scherbaum *et al.*, 2004), or the earthquake sources will need to be simulated in the hazard calculations in a way that allows the two distance metrics to be calculated correctly for each scenario (Scherbaum *et al.*, 2006). The other important difference between our model and the Gülerce and Abrahamson (2011) model is the definition of site terms, for which the latter use a continuous V_{S30}-dependent function and the former is based on generic site classes (an abiding weakness due to the lack of well-determined V_{S30} values for strong-motion sites in Europe). Nonetheless, the close agreement between the NGA and global pan-European models (e.g., Stafford *et al.*, 2008; Campbell and Bozorgnia, 2006) encourages their

complementary use for defining the hazard in Europe and the surrounding regions.

An element missing from this study is a model for the period-to-period correlations between the residuals of the V/H ratios and the residuals of the horizontal spectral ordinates, which are required to generate vertical CMS, as described by Gülerce and Abrahamson (2011). As noted in the Introduction, the vertical CMS produced from such a methodology is the most realistic way of considering the interaction between the horizontal and vertical motions that can serve for the scaling of three-component acceleration time-histories in structural analysis. This requires the generation of a compatible GMPE for the horizontal spectral ordinates, which is beyond the scope of this paper. However, because our next project is the development of a new European GMPE for the prediction of spectral ordinates for an extended range of magnitudes, which will be developed from the full dataset that was considered for this study, such a correlation model will be generated as part of that endeavor. In the meantime, we recommend the use of the model of Gülerce and Abrahamson (2011) for this purpose.

Data and Resources

The ground motions used in this study are obtained from (a) the web site www.daphne.deprem.gov.tr, operated and maintained by the Earthquake Division of the Turkish Disaster and Emergency Management Agency (DEMA), (b) the Italian strong-motion database, available at www.itaca.mi.ingv.it, and (c) the Internet-Site for European Strong-Motion Data, available at http://www.isesd.hi.is/ESD_Local/frameset.htm.

The NGA-West 2 project is available at http://peer.berkeley.edu/ngawest2/index.html.

Acknowledgments

The work was originally conducted for the PEGASOS Refinement Project, and we acknowledge the support from that project. The work to develop the strong-motion database used herein and the processing of the horizontal components of the records have been supported by the SHARE (Seismic Hazard Harmonization in Europe) project, funded under contract 226967 of the EC-Research Framework Programme FP7. Within the context of that project, we would like to express our thanks to Emrah Yenier for his assistance in the processing of the horizontal strong-motion data employed in this study. We also benefitted significantly from the constructive comments of two anonymous reviewers, who helped to improve the overall quality of the paper, and we acknowledge their contributions with gratitude.

References

Abrahamson, N. A., G. Atkinson, D. M. Boore, Y. Bozorgnia, K. Campbell, B. Chiou, I. M. Idriss, W. Silva, and R. Youngs (2008). Comparison of the NGA ground-motion relations, *Earthq. Spectra* **24,** no. 1, 45–66.

Abrahamson, N. A., and W. J. Silva (1997). Empirical response spectral attenuation relations for shallow crustal earthquakes, *Seismol. Res. Letters* **68,** no. 1, 94–127.

Abrahamson, N. A., and W. J. Silva (2008). Summary of the Abrahamson and Silva NGA ground motion relations, *Earthq. Spectra* **24,** no. 1, 67–98.

Akkar, S., and J. J. Bommer (2006). Influence of long-period filter cut-off on elastic spectral displacements, *Earthq. Eng. Struct. Dyn.* **35,** no. 9, 1145–1165.

Akkar, S., and J. J. Bommer (2007a). Prediction of elastic displacement response spectra in Europe and the Middle East, *Earthq. Eng. Struct. Dyn.* **36,** 1275–1301.

Akkar, S., and J. J. Bommer (2007b). Empirical prediction equations for peak ground velocity derived from strong-motion records from Europe and the Middle East, *Bull. Seismol. Soc. Am.* **97,** 1275–1301.

Akkar, S., and J. J. Bommer (2010). Empirical equations for the prediction of PGA, PGV and spectral accelerations in Europe, the Mediterranean region and the Middle East, *Seismol. Res. Lett.* **81,** no. 1, 195–206.

Akkar, S., Z. Çağnan, E. Yenier, Ö. Erdoğan, A. Sandıkkaya, and P. Gülkan (2010). The recently compiled Turkish strong motion database: Preliminary investigation for the seismological parameters, *J. Seismol.* **14,** no. 3, 457–479.

Akkar, S., Ö. Kale, E. Yenier, and J. J. Bommer (2011). The high-frequency limit of usable response spectral ordinates from filtered analogue and digital strong-motion accelerograms, *Earthq. Eng. Struct. Dyn.* **40,** doi 10.1002/eqe.1095.

Ambraseys, N. N., and J. Douglas (2003). Near-field horizontal and vertical earthquake ground motions, *Soil Dyn. Earthq. Eng.* **23,** no. 1, 1–18.

Ambraseys, N. N., J. Douglas, P. Smit, and S. K. Sarma (2005a). Equations for the estimation of strong ground motions from shallow crustal earthquakes using data from Europe and the Middle East: Horizontal peak ground acceleration and spectral acceleration, *Bull. Earthq. Eng.* **3,** no. 1, 1–53.

Ambraseys, N. N., J. Douglas, P. Smit, and S. K. Sarma (2005b). Equations for the estimation of strong ground motions from shallow crustal earthquakes using data from Europe and the Middle East: Vertical peak ground acceleration and spectral acceleration, *Bull. Earthq. Eng.* **3,** no. 1, 55–73.

Ambraseys, N. N., and K. A. Simpson (1996). The prediction of vertical response spectra in Europe, *Earthq. Eng. Struct. Dyn.* **25,** 401–412.

Ambraseys, N. N., K. A. Simpson, and J. J. Bommer (1996). The prediction of horizontal response spectra in Europe, *Earthq. Eng. Struct. Dyn.* **25,** 371–400.

Amirbekian, R. V., and B. A. Bolt (1998). Spectral comparison of vertical and horizontal seismic strong ground motions in alluvial basins, *Earthq. Spectra* **14,** 573–595.

Baker, J. W., and C. A. Cornell (2006). Spectral shape, epsilon and record selection, *Earthq. Eng. Struct. Dyn.* **35,** 1077–1095.

Beresnev, I. A., A. M. Nightengale, and W. J. Silva (2002). Properties of vertical ground motions, *Bull. Seismol. Soc. Am.* **92,** 3152–3164.

Berge-Thierry, C., F. Cotton, O. Scotti, D.-A. Griot-Pommera, and Y. Fukushima (2003). New empirical spectral attenuation laws for moderate European earthquakes, *J. Earthq. Eng.* **7,** no. 2, 193–222.

Beyer, K., and J. J. Bommer (2006). Relationships between median values and between aleatory variabilities for different definitions of the horizontal component of motion, *Bull. Seismol. Soc. Am.* **96,** no. 4A, 1512–1522.

Beyer, K., and J. J. Bommer (2007). Erratum to relationships between median values and between aleatory variabilities for different definitions of the horizontal component of motion, *Bull. Seismol. Soc. Am.* **97,** no. 5, 1769.

Bindi, D., L. Luzi, M. Massa, and F. Pacor (2010). Horizontal and vertical ground motion prediction equations derived from the Italian accelerometric archive (ITACA), *Bull. Earthq. Eng.* **8,** no. 5, 1209–1230.

Bindi, D., S. Parolai, H. Grosser, C. Milkereit, and E. Durukal (2007). Empirical ground-motion prediction equations for northwestern

Turkey using the aftershocks of the 1999 Kocaeli earthquake, *Geophys. Res. Lett.* **34,** L08305, doi 10.1029/2007GL029222.

Bommer, J. J., F. Scherbaum, H. Bungum, F. Cotton, F. Sabetta, and N. A. Abrahamson (2005). On the use of logic trees for ground-motion prediction equations in seismic hazard assessment, *Bull. Seismol. Soc. Am.* **95,** no. 2, 377–389.

Bommer, J. J., P. Stafford, J. Alarcon, and S. Akkar (2007). The influence of magnitude range on empirical ground-motion prediction, *Bull. Seismol. Soc. Am.* **97,** no. 6, 2152–2170.

Boore, D. M., W. B. Joyner, and T. E. Fumal (1997). Equations for estimating horizontal response spectra and peak acceleration from western North American earthquakes: A summary of recent work, *Seismol. Res. Lett.* **68,** no. 1, 128–153.

Bozorgnia, Y., and K. W. Campbell (2004a). Engineering characterization of ground motion, in *Earthquake Engineering: From Engineering Seismology to Performance-Based Engineering*, Y. Bozorgnia and V. V. Bertero (Editors), CRC Press, Boca Raton, Florida, 215–315.

Bozorgnia, Y., and K. W. Campbell (2004b). The vertical-to-horizontal spectral ratio and tentative procedures for developing simplified V/H and vertical design spectra, *J. Earthq. Eng.* **4,** no. 4, 539–561.

Bragato, P. L., and D. Slejko (2005). Empirical ground-motion relations for the Eastern Alps in the magnitude range 2.5–6.3, *Bull. Seismol. Soc. Am.* **95,** no. 1, 252–272.

Campbell, K. W. (1997). Empirical near-source attenuation relationships for horizontal and vertical components of peak ground acceleration, peak ground velocity, and pseudo-absolute acceleration response spectra, *Seismol. Res. Lett.* **68,** no. 1, 154–179.

Campbell, K. W., and Y. Bozorgnia (2003). Updated near-source ground motion (attenuation) relations for the horizontal and vertical components of peak ground acceleration and acceleration response spectra, *Bull. Seismol. Soc. Am.* **93,** no. 1, 314–331.

Campbell, K. W., and Y. Bozorgnia (2006). Next Generation Attenuation (NGA) empirical ground motion models: Can they be used in Europe, paper no. 458, *Proceedings of the First European Conference on Earthquake Engineering and Seismology*, Geneva, Switzerland, 3–8 September 2006.

Cauzzi, C., and E. Faccioli (2008). Broadband (0.05 to 20 s) prediction of displacement response based on worldwide digital records, *J. Seismol.* **12,** 453–475.

Chiou, B., R. Darragh, N. Gregor, and W. Silva (2008). NGA project strong motion database, *Earthq. Spectra* **24,** no. 1, 23–44.

Douglas, J., and D. M. Boore (2011). High-frequency filtering of strong-motion records, *Bull. Earthq. Eng.*, **9,** no. 2, 395–409.

Elnashai, A. S., and A. J. Papazoglu (1997). Procedure and spectra for analysis of RC structures subjected to vertical earthquake loads, *J. Earthq. Eng.* **1,** no. 1, 121–155.

Eurocode 8 (2004). Design of structures for earthquake resistance, part 1: General rules, seismic actions, and rules for buildings, *EN 1998-1*, European Committee for Standardization (CEN), http://www.cen.eu/cenorm/homepage.htm.

Frohlich, C., and K. D. Apperson (1992). Earthquake focal mechanisms, moment tensors, and the consistency of seismic activity near plate boundaries, *Tectonics* **11,** 279–296.

Gülerce, Z., and N. A. Abrahamson (2011). Site-specific spectra for vertical ground motion, *Earthq. Spectra*, **27,** no. 4 (in press).

Joyner, W. B., and D. M. Boore (1993). Methods for regression analysis of strong-motion data, *Bull. Seismol. Soc. Am.* **83,** 469–487.

Kalkan, E., and P. Gülkan (2004a). Empirical attenuation equations for vertical ground motion in Turkey, *Earthq. Spectra* **20,** no. 3, 853–882.

Kalkan, E., and P. Gülkan (2004b). Site-dependent spectra derived from ground motion records in Turkey, *Earthq. Spectra* **20,** no. 4, 111–1138.

Kawase, H., and K. Aki (1990). Topography effect at the critical *SV*-wave incidence: Possible explanation of damage pattern by the Whittier Narrows, California, earthquake of 1 October 1987, *Bull. Seismol. Soc. Am.* **80,** 1–30.

Lussou, P., P.-Y. Bard, F. Cotton, and Y. Fukushima (2001). Seismic design regulation codes: Contributions of K-Net data to site effect evaluations, *J. Earthq. Eng.* **5,** no. 1, 13–33.

Luzi, L., S. Hailemikael, D. Bindi, F. Pacor, F. Mele, and F. Sabetta (2008). ITACA (ITalian ACcelerometric Archive): A web portal for the dissemination of Italian strong-motion data, *Seismol. Res. Lett.* **79,** no. 1, 716–772.

Malhotra, P. K. (2006). Smooth spectra of horizontal and vertical ground motions, *Bull. Seismol. Soc. Am.* **96,** no. 2, 506–518.

Massa, M., P. Morasca, L. Moratto, S. Marzorati, G. Costa, and D. Spallarossa (2008). Empirical ground-motion equations for northern Italy using weak- and strong-motion amplitudes, frequency content, and duration parameters, *Bull. Seismol. Soc. Am.* **98,** no. 3, 1319–1342.

McGuire, R. K., W. J. Silva, and C. J. Costantino (2001). Technical basis for revision of regulatory guidance on design ground motions: Hazard- and risk-consistent ground motion spectra guidelines, *U.S. Nuclear Regulatory Commission NUREG/CR-6728*, Washington, D.C., 1020 pp

Morasca, P., F. Zolezzi, D. Spallarossa, and L. Luzi (2008). Ground motion models for the Molise region (southern Italy), *Soil Dyn. Earthq. Eng.* **28,** 198–211.

National Earthquake Hazards Reduction Program (NEHRP; 2009). *2009 NEHRP recommended seismic provisions for new buildings and other structures: Part 1, Provisions*, National Earthquake Hazards Reduction Program, Washington D.C., 373 pp.

Sabetta, F., and A. Pugliese (1996). Estimation of response spectra and simulation of nonstationary earthquake ground motions, *Bull. Seismol. Soc. Am.* **86,** no. 2, 337–352.

Sadigh, K., C. Y. Chang, J. A. Egan, F. Makdisi, and R. R. Youngs (1997). Attenuation relationships for shallow crustal earthquakes based on California strong motion data, *Seismol. Res. Lett.* **68,** no. 1, 180–189.

Scherbaum, F., J. J. Bommer, F. Cotton, H. Bungum, and F. Sabetta (2006). Ground-motion prediction in PSHA: A post-PEGASOS perspective, paper no. 1312, *Proceedings of the First European Conference on Earthquake Engineering*, Geneva, Switzerland, 3–8 September 2006.

Scherbaum, F., J. Schmedes, and F. Cotton (2004). On the conversion of source-to-site distance measures for extended earthquake source models, *Bull. Seismol. Soc. Am.* **94,** no. 3, 1053–1069.

Silva, W. (1997). Characteristics of vertical strong ground motions for applications to engineering design, in *Proceedings of the FHWA/NCEER Workshop on the National Representation of Seismic Ground Motion for New and Existing Highway Facilities*, Tech. Rept. NCEER-97-0010, M. Friedland, M. S. Power, and R. L. MayesNational Center for Earthquake Engineering Research, Buffalo, New York, 205–252.

Stafford, P. J., F. O. Strasser, and J. J. Bommer (2008). An evaluation of the applicability of the NGA models to ground motion prediction in the Euro-Mediterranean region, *Bull. Earthq. Eng.* **6,**149–177.

Thenhaus, P. C., and K. W. Campbell (2002). Seismic hazard analysis, in *Earthquake Engineering Handbook* W.-F. Chen and C. Scawthorn (Editors), CRC Press, Boca Raton, Florida, 8-1–8-43.

United States Atomic Energy Commission (USAEC; 1973). Design response spectra for seismic design of nuclear power plants, *Regulatory Guide RG 1.60*, Atomic Energy Commission, Washington, D.C.

Wells, D. L., and K. J. Coppersmith (1994). New empirical relationships among magnitude, rupture length, rupture width, rupture area, and surface displacement, *Bull. Seismol. Soc. Am.* **84,** 974–1002.

Appendix

Major features of earthquakes in the database (from Ambraseys *et al.*, 2005a; Akkar and Bommer, 2007a, 2007b,

Table A1
Earthquakes Used in the Proposed V/H Model

Date (dd/mm/yyyy)	Time	M_w	Co*	Depth, Z (km)	Style of Faulting, F	Number of Records, N_r	Distance, R_{JB} (km)†
14/06/1972	18:55:46	4.8	IT	3	*S*	2	8-11
04/11/1973	15:52:12	5.8	GR	7	*T*	1	11
06/05/1976	20:00:12	6.4	IT	12	*T*	3	10-90
09/05/1976	00:53:44	5.1	IT	20	*T*	1	32
10/05/1976	04:35:53	4.7	IT	15	*T*	1	9
11/05/1976	22:44:00	5.0	IT	13	*T*	1	13
08/06/1976	12:14:38	4.6	IT	19	*N*	3	8-20
11/06/1976	17:16:40	4.5	IT	18	*N*	2	5-6
17/06/1976	14:28:47	4.7	IT	15	*N*	3	21-27
26/06/1976	11:13:49	4.6	IT	26	*N*	3	5-11
14/07/1976	05:39:33	4.5	IT	16	*T*	2	25
11/09/1976	16:31:10	5.1	IT	10	*T*	4	4-16
11/09/1976	16:35:01	5.6	IT	9	*T*	5	10-17
13/09/1976	18:54:45	4.6	IT	14	*N*	2	11-12
15/09/1976	03:15:18	5.9	IT	2	*T*	6	5-19
15/09/1976	04:38:53	4.9	IT	21	*N*	4	4-14
15/09/1976	09:21:18	5.9	IT	21	*T*	8	5-45
15/09/1976	09:45:56	4.6	IT	27	*T*	1	5
24/11/1976	12:22:16	7.0	TR	10	*S*	1	52
03/04/1977	03:18:13	4.8	IT	9	*T*	1	9
16/09/1977	23:48:07	5.3	IT	21	*T*	5	6-11
11/03/1978	19:20:43	5.2	IT	5	*N*	3	9-54
15/04/1978	23:33:47	6.0	IT	22	*S*	4	12-37
20/06/1978	20:03:22	6.2	GR	3	*N*	1	13
16/09/1978	15:35:57	7.3	IR	4	*T*	1	8
09/04/1979	02:10:21	5.4	MO	13	*T*	1	29
15/04/1979	06:19:41	6.9	MO	12	*T*	8	3-96
15/04/1979	14:43:06	5.8	MO	7	*T*	3	22-41
24/05/1979	17:23:18	6.2	MO	5	*T*	5	15-35
19/09/1979	21:35:37	5.8	IT	6	*N*	4	9-39
01/01/1980	16:42:39	6.9	PO	5	*S*	1	80
05/01/1980	14:32:26	4.8	IT	21	*T*	1	17
07/06/1980	18:35:01	4.6	IT	30	*N*	3	12-26
11/08/1980	09:15:59	5.2	GR	5	*T*	1	13
26/09/1980	04:19:21	5.0	GR	42	*N*	1	10
23/11/1980	18:34:53	6.9	IT	15	*N*	14	7-86
16/01/1981	00:37:45	5.2	IT	11	*N*	12	9-25
14/02/1981	17:27:46	4.9	IT	10	*T*	2	27-45
24/02/1981	20:53:39	6.2	GR	18	*N*	2	8-10
25/02/1981	02:35:53	5.9	GR	30	*N*	1	19
10/03/1981	15:16:20	5.4	GR	10	*T*	2	7-21
17/10/1982	06:45:37	4.6	IT	6	*N*	1	23
17/01/1983	12:41:31	6.3	GR	14	*T*	2	67-90
31/01/1983	15:27:02	5.4	GR	39	*N*	1	52
23/03/1983	23:51:08	5.8	GR	13	*S*	1	70
06/08/1983	15:43:53	6.6	AS	22	*S*	1	76
26/08/1983	12:52:09	5.2	GR	3	*S*	2	11-35
09/11/1983	16:29:52	5.0	IT	28	*T*	1	21
29/04/1984	05:03:00	5.6	IT	6	*N*	4	10-47
07/05/1984	17:49:43	5.9	IT	21	*N*	7	13-44
11/05/1984	10:41:48	5.5	IT	12	*N*	7	9-37
11/05/1984	11:26:16	4.9	IT	18	*N*	2	10-16
11/05/1984	13:14:56	5.0	IT	14	*N*	3	7-21
11/05/1984	16:39:18	5.0	IT	17.5	*N*	2	9-14
24/06/1984	14:30:51	4.9	SP		*N*	1	29
09/07/1984	18:57:12	5.2	GR	5.0	*N*	1	21
09/07/1984	18:57:12	5.2	GR	5.0	*N*	1	21
24/08/1984	06:02:26	5.3	DS	18.0	*S*	1	22
30/04/1985	18:14:13	5.6	GR	25.5	*N*	1	15
09/11/1985	23:30:43	5.2	GR	18.0	*N*	2	19-51
05/05/1986	03:35:38	6.0	TR	4.4	*S*	1	24
13/09/1986	17:24:34	6.0	GR	27.6	*N*	1	0
15/09/1986	11:41:28	5.3	GR	10.0	*N*	3	14-21
27/02/1987	23:34:52	5.5	GR	5.4	*N*	1	35
24/04/1987	02:30:29	4.9	IT	23.5	*S*	2	5-18
02/05/1987	20:43:55	4.7	IT	23.7	*S*	2	7-19
25/05/1987	11:31:56	6.0	IC	8.0	*S*	4	24-45
10/06/1987	14:50:12	5.3	GR	30.0	*T*	1	9
24/04/1988	10:10:33	4.5	GR	3.7	*T*	1	16
18/05/1988	05:17:42	5.5	GR	20.7	*T*	2	12-23
05/07/1988	20:34:52	5.5	GR	17.4	*N*	1	22
16/10/1988	12:34:05	5.6	GR	25.0	*S*	3	11-49
07/12/1988	07:41:24	6.7	AR	6.0	*T*	1	20
22/12/1988	09:56:50	4.9	GR	37.8	*N*	1	6
07/06/1989	19:45:54	5.2	GR	25.0	*S*	1	24
31/08/1989	21:29:31	4.8	GR	32.0	*N*	1	21
29/10/1989	19:09:13	5.9	AL	6.0	*T*	1	61
05/05/1990	07:21:20	5.8	IT	22.5	*S*	3	27-39
05/05/1990	07:38:12	4.8	IT	11.3	*S*	1	34
20/06/1990	21:00:08	7.4	IR	19.0	*S*	4	49-92
13/12/1990	00:24:26	5.6	IT	7.0	*S*	5	31-80
16/12/1990	15:45:51	5.4	AR	28.0	*S*	4	15-44
21/12/1990	06:57:43	5.9	GR	13.3	*N*	2	31
19/03/1991	12:09:23	5.7	GR	6.8	*N*	1	65

(*continued*)

Table A1 (*Continued*)

(*continued*)

Table A1 (*Continued*)

Date (dd/mm/yyyy)	Time	M_w	Co*	Depth, Z (km)	Style of Faulting, F	Number of Records, N_r	Distance, R_{JB} (km)†
03/05/1991	20:19:39	5.6	CU	15.0	*T*	4	11-28
26/05/1991	12:26:01	5.1	IT	30.3	*S*	2	32-42
15/06/1991	00:59:20	6.0	CU	6.0	*T*	3	37-56
23/01/1992	04:24:17	5.4	GR	24.9	*T*	2	14-42
13/03/1992	17:18:40	6.6	TR	22.6	*S*	2	3-63
15/03/1992	16:16:16	5.9	TR	28.5	*S*	2	26-42
06/11/1992	19:08:09	6.0	AS	17.2	*S*	1	38
18/11/1992	21:10:41	5.9	GR	15.0	*N*	1	25
15/02/1993	14:49:18	4.6	GR	7.1	*S*	1	17
26/03/1993	11:45:16	5.1	GR	31.7	*S*	2	2-15
26/03/1993	11:56:14	5.1	GR	26.4	*S*	2	4-13
26/03/1993	11:58:15	5.5	GR	45.2	*S*	1	24
29/04/1993	07:54:29	5.1	GR	10.0	*S*	1	3
13/06/1993	23:26:40	5.6	GR	19.6	*T*	1	33
14/07/1993	12:31:50	5.5	GR	12.4	*S*	5	9-30
14/07/1993	12:39:13	4.5	GR	30.0	*S*	2	5-6
04/11/1993	05:18:37	5.3	GR	10.0	*N*	3	10-19
23/12/1993	14:22:34	5.2	SP	18.0	*N*	1	6
04/01/1994	08:03:15	5.2	SP	16.0	*N*	2	24-41
25/02/1994	02:30:50	5.5	GR	23.5	*S*	5	12-29
27/02/1994	22:34:52	4.5	GR	10.0	*T*	2	21-28
20/06/1994	09:09:03	5.9	IR	9.0	*S*	6	7-58
29/11/1994	14:30:30	5.2	GR	21.0	*S*	2	15-17
03/05/1995	21:36:54	4.9	GR	20	*N*	1	27
03/05/1995	21:43:27	5.0	GR	24	*N*	2	27-33
04/05/1995	00:34:11	5.3	GR	14	*N*	3	28-43
13/05/1995	08:47:15	6.1	GR	14	*N*	6	14-78
14/05/1995	14:46:57	4.8	GR	19	*N*	1	8
15/05/1995	04:13:57	5.4	GR	26	*N*	3	9-27
16/05/1995	23:57:28	5.2	GR	25	*N*	2	9-21
19/05/1995	06:48:49	5.4	GR	10	*N*	4	15-28
19/05/1995	07:36:19	4.6	GR	8	*N*	1	18
20/05/1995	21:06:25	4.9	GR	27	*S*	2	7-8
06/06/1995	04:36:00	5.1	GR	24	*N*	4	10-26
11/06/1995	18:51:48	5.1	GR	27	*N*	3	1-9
15/06/1995	00:15:51	6.1	GR	3	*N*	4	7-35
25/06/1995	01:05:32	4.5	GR	11	*N*	1	6
17/07/1995	23:18:15	5.5	GR	22	*N*	1	22
18/08/1995	00:52:23	5.1	TR	18	*N*	1	32
30/09/1995	10:14:34	5.2	IT	27	*T*	3	22-46
01/10/1995	15:57:13	6.4	TR	5	*N*	3	0-87
22/11/1995	04:15:12	7.1	EG	13	*S*	1	48
23/11/1995	18:07:13	5.7	EG	24	*S*	1	32
05/12/1995	18:49:32	5.8	TR	26	*S*	1	59

(*continued*)

Table A1 (*Continued*)

Date (dd/mm/yyyy)	Time	M_w	Co*	Depth, Z (km)	Style of Faulting, F	Number of Records, N_r	Distance, R_{JB} (km)†
05/12/1995	18:52:40	5.8	TR	10	*S*	1	66
26/12/1995	06:19:38	4.5	EG	12	*S*	1	81
02/04/1996	07:59:26	5.4	GR	15	*N*	1	65
15/07/1996	00:13:30	4.7	FR	4	*S*	1	21
11/08/1996	11:43:45	4.9	GR	48	*S*	1	8
14/08/1996	01:55:03	5.7	TR	12	*S*	1	43
14/08/1996	02:59:41	5.6	TR	3	*S*	1	44
02/09/1996	19:07:01	4.6	SP	17	*N*	1	1
09/10/1996	13:10:50	6.8	CY	19	*S*	1	84
15/10/1996	09:56:01	5.4	IT	26	*T*	3	13-28
13/01/1997	10:19:25	5.7	CY	15	*S*	2	53-77
22/01/1997	17:57:20	5.7	TR	45	*N*	1	19
24/02/1997	07:09:50	4.6	SP	14	*N*	10	2-32
28/02/1997	00:03:52	5.2	TR	5	*S*	1	40
26/03/1997	04:22:51	5.1	LE	5	*N*	1	75
26/04/1997	22:18:34	4.9	GR	45	*S*	1	26
02/07/1997	12:53:07	4.5	SP	25	*S*	2	33-54
03/09/1997	22:07:29	4.9	IT	3	*N*	2	10-21
26/09/1997	00:33:12	5.7	IT	4	*N*	11	0-78
26/09/1997	09:40:25	6.0	IT	10	*N*	14	0-66
26/09/1997	13:30:52	4.5	IT	14	*N*	1	25
27/09/1997	08:08:08	4.7	IT	9	*N*	2	2-15
02/10/1997	10:59:56	4.7	IT	8	*N*	3	2-15
03/10/1997	08:55:22	5.2	IT	12	*N*	9	6-36
04/10/1997	16:13:33	4.9	IT	1	*N*	4	7-18
06/10/1997	23:24:53	5.4	IT	4	*N*	10	4-66
07/10/1997	01:24:34	4.6	IT	9	*N*	4	8-19
07/10/1997	05:09:57	4.9	IT	4	*N*	7	5-39
12/10/1997	05:06:07	4.6	TR	60	*T*	1	11
12/10/1997	11:08:36	5.2	IT	0	*N*	13	7-53
13/10/1997	13:09:21	4.8	IT	8	*N*	3	9-25
14/10/1997	15:23:09	5.6	IT	7	*N*	16	7-74
16/10/1997	04:52:55	4.5	IT	4	*N*	1	6
16/10/1997	12:00:31	4.8	IT	1	*S*	5	3-11
19/10/1997	16:00:18	4.7	IT	8	*N*	5	7-15
05/11/1997	21:10:28	5.6	GR	24	*N*	1	28
09/11/1997	19:07:33	5.0	IT	4	*N*	7	4-34
18/11/1997	13:07:41	6.0	IS	10	*T*	3	39-65
07/02/1998	00:59:44	4.9	IT	4	*N*	7	5-18
05/03/1998	01:45:08	4.8	TR	23	*N*	2	48-100
21/03/1998	16:45:09	5.0	IT	1	*N*	9	6-23
28/03/1998	00:29:57	4.5	TR	6	*S*	1	42
03/04/1998	07:26:36	5.1	IT	2	*N*	12	5-36
03/04/1998	07:59:51	4.7	IT	4	*N*	6	2-19

(*continued*)

Table A1 (*Continued*)

Date (dd/mm/yyyy)	Time	M_w	Co*	Depth, Z (km)	Style of Faulting, F	Number of Records, N_r	Distance, R_{JB} (km)†
04/04/1998	16:16:47	5.2	TR	19	*N*	2	42-88
05/04/1998	15:52:20	5.0	IT	10	*N*	11	6-37
12/04/1998	10:55:33	5.6	IT	8	*S*	1	24
13/04/1998	15:14:33	5.2	TR	15	*S*	1	76
09/05/1998	15:38:00	5.1	TR	27	*S*	2	48-53
04/06/1998	21:36:54	5.4	IC		*S*	6	6-49
27/06/1998	13:55:52	6.2	TR	47	*S*	1	40
04/07/1998	02:15:46	5.4	TR	55	*S*	1	52
09/07/1998	05:19:07	6.1	PO	10	*S*	2	11-72
09/07/1998	17:36:46	5.0	TR	17	*N*	1	75
09/09/1998	11:28:00	5.6	IT	29	*N*	3	10-34
08/10/1998	20:48:06	4.6	TR	18	*S*	1	24
10/11/1998	05:39:32	4.8	TR	24	*S*	1	34
13/11/1998	10:38:34	5.1	IC		*S*	2	9-11
20/12/1998	03:21:14	4.8	TR	10	*S*	1	55
14/02/1999	11:45:53	4.7	IT	21	*N*	2	11-24
11/06/1999	05:25:18	4.9	TR	23	*N*	1	94
07/07/1999	17:16:12	4.7	IT	12	*N*	1	10
20/07/1999	04:22:40	4.8	TR	41	*S*	1	7
24/07/1999	16:05:50	5.0	TR	10	*S*	1	38
25/07/1999	06:56:54	5.2	TR	15	*S*	1	35
17/08/1999	00:01:40	7.6	TR	17	*S*	18	1-97
17/08/1999	01:07:52	4.9	TR	22	*S*	1	86
17/08/1999	02:50:47	5.1	TR	11	*S*	1	94
19/08/1999	01:52	4.7	TR	28	*S*	1	49
19/08/1999	14:16:00	4.7	TR	3	*N*	1	46
19/08/1999	15:17:79	5.1	TR	12	*S*	3	41-48
20/08/1999	10:00:19	5.1	TR	26	*S*	1	86
22/08/1999	11:12:04	4.6	TR	28	*S*	1	51
29/08/1999	10:15:04	4.9	TR	14	*N*	4	6-57
31/08/1999	08:10:63	5.1	TR	4	*S*	14	14-89
31/08/1999	08:33:25	4.5	TR	6	*N*	2	37-87
07/09/1999	11:56:51	6.0	GR	17	*N*	11	5-13
09/09/1999	08:15:35	4.8	TR	24	*N*	1	52
13/09/1999	11:55:30	5.8	TR	10	*S*	23	9-100
24/09/1999	19:08:04	5.0	TR	12	*S*	1	97
29/09/1999	00:13:07	5.2	TR	12	*S*	1	86
05/10/1999	00:53:28	5.2	TR	17	*N*	1	76
07/11/1999	16:54:41	5.1	TR	7	*T*	7	5-27
11/11/1999	14:41:23	5.6	TR	8	*S*	12	31-82
12/11/1999	16:57:20	7.1	TR	10	*S*	15	0-98
12/11/1999	17:17:00	5.0	TR	9	*S*	7	8-54
12/11/1999	17:26:15	4.7	TR	10	*S*	1	8
12/11/1999	17:47:16	5.0	TR	20	*S*	1	63

(*continued*)

Table A1 (*Continued*)

Date (dd/mm/yyyy)	Time	M_w	Co*	Depth, Z (km)	Style of Faulting, F	Number of Records, N_r	Distance, R_{JB} (km)†
12/11/1999	20:04:44	4.8	TR	10	*S*	3	27-45
12/11/1999	21:38:32	4.7	TR	12	*S*	6	11-40
12/11/1999	22:20:53	5.0	TR	25	*S*	6	30-63
13/11/1999	00:54:43	5.0	TR	5	*N*	5	10-48
15/11/1999	16:26:58	4.5	TR	11	*S*	5	18-39
16/11/1999	17:51:18	5.0	TR	5	*S*	5	47-81
19/11/1999	19:59:08	4.9	TR	5	*N*	4	15-55
20/11/1999	08:44:13	5.1	TR	7	*S*	3	51-56
21/11/1999	22:27:32	4.7	TR	9	*S*	3	53-58
13/12/1999	19:13:40	4.7	TR	14	*S*	1	10
29/12/1999	20:42:34	5.1	SW	5	*N*	12	8-69
29/12/1999	20:42:35	4.8	IT	5	*N*	1	14
31/12/1999	04:55:54	4.5	IT	15	*N*	8	9-21
20/01/2000	10:35:59	4.9	TR	13	*S*	6	15-60
14/02/2000	06:56:35	5.3	TR	10	*S*	2	49-55
01/04/2000	18:08:03	4.5	IT	2	*N*	1	2
02/04/2000	11:41:09	4.6	TR	28	*S*	1	66
02/04/2000	18:57:40	4.5	TR	9	*S*	1	16
06/04/2000	17:40:37	4.6	SW	5	*N*	5	10
21/04/2000	12:23:06	5.4	TR	20	*N*	3	23-85
10/05/2000	16:52:11	4.8	IT	23	*T*	1	8
06/06/2000	02:41:51	6.0	TR	10	*N*	3	8-91
06/06/2000	05:59:40	4.6	TR	8	*S*	1	24
08/06/2000	21:27:56	4.9	TR	33	*N*	1	9
17/06/2000	15:40:41	6.5	IC	15	*S*	20	5-76
21/06/2000	00:51:48	6.4	IC		*S*	13	2-53
01/08/2000	04:35:46	5.1	PO	13	*S*	1	39
21/08/2000	17:14:28	4.8	IT	24	*N*	1	6
23/08/2000	13:41:28	5.3	TR	11	*S*	5	14-94
08/09/2000	05:46:46	4.7	TR	5	*S*	1	34
04/10/2000	02:33:58	5.0	TR	3	*N*	2	10-90
04/10/2000	07:58:50	4.6	TR	2	*N*	1	24
15/11/2000	15:05:34	5.5	TR	48	*S*	1	37
15/11/2000	16:06:03	5.0	TR	45	*T*	1	44
02/02/2001	09:51:39	4.6	TR	18	*N*	1	5
25/02/2001	18:34:41	4.9	FR	10	*T*	1	35
08/04/2001	06:12:24	4.9	GR	14	*N*	2	16-20
29/05/2001	13:14:27	4.9	TR	20	*S*	1	34
29/05/2001	14:15:53	4.9	TR	10	*T*	1	60
22/06/2001	11:54:51	5.2	TR	7	*N*	1	34
23/06/2001	12:18:21	4.8	TR	8	*S*	1	28
25/06/2001	13:28:46	5.4	TR	10	*N*	2	41-74
10/07/2001	21:42:04	5.4	TR	23	*S*	1	31
17/07/2001	15:06:12	5.1	IT	2	*S*	2	19-69

(*continued*)

Table A1 (*Continued*)

Date (dd/mm/yyyy)	Time	M_w	Co*	Depth, Z (km)	Style of Faulting, F	Number of Records, N_r	Distance, R_{JB} (km)†
26/08/2001	00:41:14	5.2	TR	9	*S*	2	93-99
16/09/2001	02:00:46	5.5	GR	10	*N*	1	99
01/10/2001	06:36:22	4.6	IT	6	*N*	1	23
26/11/2001	00:56:55	4.7	IT	6	*N*	2	3-9
29/11/2001	19:36:48	4.8	TR	10	*S*	1	30
02/12/2001	04:11:46	4.8	TR	20	*T*	1	14
21/01/2002	14:34:24	4.8	TR	27	*N*	2	59-89
03/02/2002	07:11:28	6.5	TR	22	*N*	1	52
03/02/2002	09:26:43	5.8	TR	25	*N*	1	31
17/04/2002	06:42:54	4.9	IT	4	*S*	4	25-53
25/04/2002	17:41:22	5.0	GE	10	*S*	1	7
22/06/2002	02:58:21	6.5	IR	10	*T*	2	28-53
30/07/2002	12:20:24	4.7	TR	6	*N*	1	25
27/10/2002	02:50:27	4.9	IT	0	*S*	2	23-36
29/10/2002	10:02:23	4.9	IT	6	*S*	1	20
31/10/2002	10:32:59	5.7	IT	25	*S*	6	32-97
01/11/2002	15:09:02	5.7	IT	21	*S*	7	20-97
12/11/2002	09:27:48	4.6	IT	29	*S*	9	5-34
19/11/2002	01:25:35	4.8	TR	10	*S*	1	36
14/12/2002	01:02:44	4.8	TR	29	*N*	1	17
26/01/2003	19:57:04	4.7	IT	6	*N*	2	6-13
27/01/2003	05:26:23	6.0	TR	10	*S*	2	51-84
22/02/2003	20:41:06	4.7	FR	11	*S*	3	72-98
20/03/2003	12:25:33	4.6	TR	14	*S*	2	40-49
10/04/2003	00:40:14	5.7	AS	10	*S*	1	42
10/04/2003	00:40:16	5.7	TR	11	*S*	1	33
11/04/2003	09:26:58	4.8	IT	16	*S*	1	17
17/04/2003	22:34:34	5.2	TR	12	*N*	1	59
01/05/2003	00:27:04	6.3	TR	10	*S*	1	2
08/05/2003	01:44:19	4.9	TR	9	*S*	1	12
10/05/2003	15:44:49	4.8	TR	10	*S*	2	21
12/05/2003	05:01:19	4.5	TR	10	*S*	1	11
01/06/2003	15:45:18	4.8	IT	16	*T*	6	6-96
09/06/2003	17:44:03	4.8	TR	9	*N*	4	91-98
22/06/2003	23:46:19	4.6	TR	8	*N*	2	72-93
06/07/2003	19:10:43	5.7	TR	17	*S*	1	44
06/07/2003	20:10:13	5.2	TR	17	*S*	1	41
06/07/2003	20:48:55	4.6	TR	10	*S*	1	44
09/07/2003	22:08:48	4.5	TR	18	*S*	1	49
09/07/2003	22:31:40	4.8	TR	18	*S*	1	54
10/07/2003	01:26:16	4.6	TR	10	*S*	1	53
13/07/2003	01:48:20	5.5	TR	13	*S*	1	55
23/07/2003	04:56:05	5.3	TR	28	*N*	3	30-74
26/07/2003	01:00:57	4.9	TR	5	*S*	5	19-78

(*continued*)

Table A1 (*Continued*)

Date (dd/mm/yyyy)	Time	M_w	Co*	Depth, Z (km)	Style of Faulting, F	Number of Records, N_r	Distance, R_{JB} (km)†
26/07/2003	08:36:10	5.4	TR	21	*N*	3	11-76
26/07/2003	13:31:37	4.9	TR	7	*N*	4	17-74
28/07/2003	17:19:06	4.5	TR	5	*N*	1	20
14/09/2003	21:42:53	5.3	IT	16	*T*	6	12-69
23/12/2003	12:23:36	4.8	TR	15	*N*	1	57
30/12/2003	05:31:38	4.5	IT	15	*S*	8	14-88
06/01/2004	10:39:10	4.7	TR	6	*S*	1	62
26/02/2004	04:13:56	4.9	TR	5	*N*	2	33-44
03/03/2004	14:38:39	4.6	TR	7	*N*	1	19
28/03/2004	03:51:09	5.6	TR	5	*S*	1	49
16/05/2004	03:30:49	4.6	TR	11	*S*	3	34-47
31/05/2004	22:50:10	4.7	TR	15	*S*	1	11
15/06/2004	12:02:40	5.2	TR	7	*S*	1	54
16/05/2004	03:30:49	4.6	TR	11	*S*	3	34-47
31/05/2004	22:50:10	4.7	TR	15	*S*	1	11
15/06/2004	12:02:40	5.2	TR	7	*S*	1	54
12/07/2004	13:04:06	5.2	IT	6	*T*	4	28-90
18/07/2004	13:04:00	4.6	TR	9	*S*	1	53
03/08/2004	05:33:37	4.8	TR	12	*N*	1	31
03/08/2004	09:41:15	4.5	TR	7	*N*	1	36
03/08/2004	13:11:32	5.2	TR	10	*N*	1	33
04/08/2004	03:01:07	5.5	TR	10	*N*	1	33
04/08/2004	03:49:34	4.7	TR	19	*N*	1	35
04/08/2004	04:19:49	5.2	TR	10	*N*	1	38
04/08/2004	04:26:22	5.2	TR	13	*N*	1	38
04/08/2004	14:18:50	5.3	TR	10	*N*	1	34
11/08/2004	15:48:26	5.6	TR	7	*S*	2	33-78
26/09/2004	21:03:16	4.5	TR	14	*T*	1	16
20/12/2004	23:02:15	5.3	TR	13	*N*	5	16-98
10/01/2005	23:48:51	5.4	TR	16	*N*	2	30-40
10/01/2005	23:53:40	5.3	TR	12	*N*	1	37
11/01/2005	00:02:20	4.7	TR	16	*N*	1	37
11/01/2005	04:35:58	5.0	TR	15	*N*	1	25
14/01/2005	19:08:11	4.7	TR	15	*N*	2	22-32
17/01/2005	17:33:32	4.6	TR	7	*S*	1	35
23/01/2005	22:36:06	5.8	TR	12	*S*	1	75
25/01/2005	16:44:15	5.8	TR	23	*S*	1	98
29/01/2005	18:52:30	4.9	TR	20	*S*	1	46
30/01/2005	16:23:49	5.3	TR	28	*S*	1	49
12/03/2005	07:36:11	5.6	TR	7	*S*	1	62
14/03/2005	01:55:57	5.8	TR	10	*S*	2	50-64
14/03/2005	04:58:07	4.9	TR	16	*S*	1	61
23/03/2005	21:44:52	5.6	TR	12	*S*	2	51-65
23/03/2005	23:43:42	5.1	TR	9	*S*	1	65

(*continued*)

Table A1 (*Continued*)

Date (dd/mm/yyyy)	Time	M_w	Co*	Depth, Z (km)	Style of Faulting, F	Number of Records, N_r	Distance, R_{JB} (km)†
09/04/2005	19:28:23	4.8	TR	11	*S*	1	29
06/06/2005	07:41:30	5.6	TR	11	*S*	3	45-64
09/08/2005	01:28:06	4.7	TR	4	*S*	1	31
20/08/2005	10:08:44	4.7	TR	11	*N*	1	26
17/10/2005	05:45:18	5.5	TR	21	*S*	2	53-74
17/10/2005	05:59:22	4.8	TR	4	*S*	1	62
17/10/2005	08:28:52	5.1	TR	2	*S*	1	58
17/10/2005	08:34:44	5.2	TR	4	*S*	1	60
17/10/2005	09:46:56	5.8	TR	19	*S*	2	51-72
17/10/2005	09:55:31	5.2	TR	11	*S*	1	56
17/10/2005	12:43:28	5.0	TR	21	*S*	1	66
18/10/2005	16:00:47	5.0	TR	26	*S*	1	69
20/10/2005	21:40:02	5.8	TR	15	*S*	2	54-75
20/10/2005	21:43:59	4.9	TR	5	*S*	1	54
31/10/2005	05:26:39	4.8	TR	16	*S*	1	60
31/10/2005	06:48:22	4.8	TR	2	*S*	1	59
02/11/2005	04:27:12	4.8	TR	3	*S*	1	68
26/11/2005	15:56:57	5.1	TR	19	*N*	1	48
10/12/2005	00:09:46	5.4	TR	19	*S*	2	62-65
08/02/2006	04:07:42	4.9	TR	7	*S*	1	98
18/04/2006	01:21:44	4.5	TR	24	*N*	1	24
03/06/2006	14:40:26	4.7	TR	9	*S*	1	37
02/07/2006	19:39:39	5.0	TR	15	*S*	2	63-64
09/10/2006	05:01:35	4.7	TR	11	*N*	1	70
12/10/2006	03:20:07	4.6	TR	6	*N*	1	25
19/10/2006	21:00:48	4.7	TR	9	*S*	1	44
20/10/2006	18:15:26	5.1	TR	17	*S*	4	33-98
24/10/2006	14:00:22	5.2	TR	8	*N*	10	7-97
01/11/2006	21:19:44	4.8	TR	5	*N*	3	48-66
19/12/2006	19:15:38	4.9	TR	19	*S*	7	34-91
21/01/2007	07:38:58	5.1	TR	3	*S*	1	17
23/01/2007	21:21:58	4.9	TR	27	*N*	5	22-73
26/01/2007	08:20:35	4.9	TR	9	*S*	1	34
25/08/2007	22:05:48	5.3	TR	16	*S*	1	1
29/10/2007	09:23:16	5.3	TR	29	*N*	6	0-99
09/11/2007	01:43:05	5.2	TR	16	*S*	1	100
16/11/2007	09:08:22	5.1	TR	22	*N*	1	37
23/12/2008	15:24:21	5.4	IT	27	*T*	17	32-91
23/12/2008	21:58:25	4.9	IT	31	*T*	10	9-91
06/04/2009	01:32:39	6.3	IT	9	*N*	18	0-96
06/04/2009	02:37:04	5.1	IT	10	*N*	13	5-99
06/04/2009	23:15:37	5.1	IT	9	*N*	15	8-93
07/04/2009	09:26:28	5.0	IT	10	*N*	18	4-65
07/04/2009	17:47:37	5.6	IT	15	*N*	29	5-98
07/04/2009	21:34:29	4.6	IT	7	*N*	18	1-63
09/04/2009	00:52:59	5.4	IT	15	*N*	27	9-83
09/04/2009	19:38:16	5.3	IT	17	*N*	25	10-89
13/04/2009	21:14:24	5.1	IT	8	*N*	16	16-66

*Co is the country or region where the earthquake occurred: AS, Aegean Sea; AL, Algeria; AR, Armenia; CU, Caucasus; CY, Cyprus; DS, Dead Sea; EG, Egypt; FR, France; GE, Georgia; GR, Greece; IC, Iceland; IS, Ionian Sea; IR, Iran; IT, Italy; LE, Lebanon; MO, Montenegro; PO, Portugal; SP, Spain; SW, Switzerland; TR, Turkey.

†R_{JB} is the Joyner–Boore distance range of the records used from a given earthquake.

Table A2
Regression Coefficients of the Proposed V/H Model

c	b_1	b_2	b_4	b_6	b_7	b_8	b_9	b_{10}	σ_{intra}	σ_{inter}	σ_{total}
0.00	−0.102010	−0.010910	−0.029480	5.0	−0.03110	−0.004170	−0.024340	−0.05460	0.1562	0.0424	0.1619
0.02	−0.048240	−0.011520	−0.059370	5.0	−0.01705	−0.003201	−0.018660	−0.05341	0.1583	0.0471	0.1652
0.03	0.006860	−0.006960	−0.100040	5.0	−0.01345	−0.003028	−0.022320	−0.05485	0.1617	0.0525	0.1700
0.04	0.044360	−0.002150	−0.123290	5.0	−0.01172	−0.003033	−0.035170	−0.06624	0.1653	0.0546	0.1741
0.05	−0.009720	0.012190	−0.122630	5.0	−0.01155	−0.003194	−0.042690	−0.05713	0.1749	0.0504	0.1820
0.10	−0.305180	0.027400	0.026440	5.0	−0.02317	−0.005600	−0.032170	−0.06561	0.1862	0.0582	0.1951
0.15	−0.299270	0.012260	0.029540	5.0	−0.03495	−0.008685	−0.033170	−0.08852	0.1826	0.0685	0.1950
0.20	−0.343790	0.000270	0.039380	5.0	−0.04458	−0.011770	−0.007000	−0.02472	0.1834	0.0627	0.1938
0.25	−0.350190	−0.007500	0.057070	5.0	−0.05420	−0.018815	0.021050	−0.00783	0.1959	0.0352	0.1990
0.30	−0.346760	−0.007200	0.059830	5.0	−0.07692	−0.025860	0.031490	−0.00890	0.1981	0.0307	0.2005
0.35	−0.323000	−0.012430	0.060130	5.0	−0.08727	−0.036910	0.030930	0.00753	0.2055	0.0406	0.2095
0.40	−0.249300	−0.027300	0.064700	5.0	−0.09193	−0.045150	0.039740	0.00894	0.2067	0.0399	0.2105
0.45	−0.227530	−0.033210	0.075400	5.0	−0.08656	−0.047410	0.048960	−0.00396	0.2052	0.0530	0.2119
0.50	−0.224780	−0.032060	0.073880	5.0	−0.09167	−0.049760	0.047410	−0.00851	0.2042	0.0582	0.2123
0.55	−0.241300	−0.029450	0.080390	5.0	−0.10102	−0.058450	0.056740	−0.00148	0.2030	0.0635	0.2127
0.60	−0.235650	−0.030770	0.087420	5.0	−0.10153	−0.068360	0.052990	−0.00454	0.2009	0.0670	0.2118
0.65	−0.257720	−0.025290	0.081440	5.0	−0.10546	−0.066660	0.063530	0.01171	0.1997	0.0594	0.2083
0.70	−0.226410	−0.026900	0.069250	5.0	−0.10667	−0.060350	0.063670	0.02085	0.1991	0.0500	0.2053
0.75	−0.203960	−0.029290	0.067780	5.0	−0.10742	−0.054570	0.051670	0.01998	0.1974	0.0549	0.2049
0.80	−0.205370	−0.030950	0.075530	5.0	−0.10199	−0.053420	0.054050	0.02308	0.1934	0.0599	0.2025
0.85	−0.207180	−0.028480	0.069170	5.0	−0.10328	−0.052240	0.056430	0.02076	0.1933	0.0593	0.2022
0.90	−0.239480	−0.022940	0.073060	5.0	−0.10244	−0.049860	0.060030	0.03429	0.1929	0.0543	0.2004
0.95	−0.252610	−0.017090	0.067400	5.0	−0.10631	−0.058810	0.059610	0.03540	0.1925	0.0470	0.1982
1.00	−0.252090	−0.015030	0.068510	5.0	−0.10982	−0.070270	0.053800	0.03236	0.1934	0.0472	0.1991
1.05	−0.233610	−0.013750	0.057400	5.0	−0.11105	−0.073680	0.052070	0.03228	0.1974	0.0326	0.2001
1.10	−0.226760	−0.012850	0.048820	5.0	−0.10924	−0.071040	0.054750	0.02673	0.2003	0.0310	0.2027
1.15	−0.214620	−0.014480	0.050010	5.0	−0.11110	−0.063410	0.050160	0.01594	0.1985	0.0366	0.2018
1.20	−0.201520	−0.015650	0.047020	5.0	−0.11085	−0.060250	0.047970	0.01931	0.1948	0.0393	0.1987
1.25	−0.188610	−0.016820	0.047070	5.0	−0.11613	−0.061980	0.045360	0.01879	0.1923	0.0441	0.1973
1.30	−0.185200	−0.016950	0.048580	5.0	−0.11545	−0.065560	0.041390	0.02436	0.1921	0.0426	0.1968
1.35	−0.169760	−0.018370	0.048080	5.0	−0.11470	−0.067380	0.034550	0.02311	0.1940	0.0383	0.1977
1.40	−0.151650	−0.020220	0.044360	5.0	−0.11301	−0.065790	0.031590	0.02016	0.1943	0.0358	0.1976
1.45	−0.137240	−0.021750	0.042340	5.0	−0.11314	−0.066330	0.031880	0.02742	0.1930	0.0338	0.1959
1.50	−0.138290	−0.021350	0.043240	5.0	−0.11714	−0.069300	0.038330	0.02899	0.1946	0.0349	0.1977
1.55	−0.139080	−0.020580	0.043030	5.0	−0.11940	−0.073090	0.041580	0.02972	0.1972	0.0381	0.2008
1.60	−0.148060	−0.020070	0.049910	5.0	−0.12399	−0.078900	0.045540	0.03380	0.1997	0.0403	0.2037
1.65	−0.170620	−0.018270	0.058830	5.0	−0.12822	−0.086390	0.055370	0.04343	0.2012	0.0446	0.2061
1.70	−0.174700	−0.018580	0.063650	5.0	−0.12768	−0.089240	0.056480	0.04948	0.2012	0.0484	0.2069
1.75	−0.180080	−0.017810	0.065370	5.0	−0.12801	−0.092530	0.056840	0.05499	0.2007	0.0518	0.2073
1.80	−0.182010	−0.016820	0.063930	5.0	−0.12778	−0.094840	0.057700	0.06706	0.1997	0.0543	0.2070
1.85	−0.165220	−0.019090	0.064050	5.0	−0.12972	−0.093750	0.057180	0.06941	0.1979	0.0588	0.2065
1.90	−0.174020	−0.017670	0.065270	5.0	−0.13040	−0.094030	0.060770	0.07396	0.1976	0.0612	0.2069
1.95	−0.174950	−0.017440	0.065280	5.0	−0.12925	−0.092840	0.061450	0.07768	0.1958	0.0624	0.2055
2.00	−0.164020	−0.019200	0.063130	5.0	−0.12645	−0.090330	0.063890	0.08354	0.1942	0.0619	0.2038
2.05	−0.155500	−0.021280	0.062620	5.0	−0.12040	−0.084890	0.067070	0.09018	0.1926	0.0631	0.2027
2.10	−0.151600	−0.022160	0.062000	5.0	−0.11798	−0.080970	0.068580	0.09122	0.1907	0.0625	0.2007
2.15	−0.154570	−0.022190	0.062990	5.0	−0.11662	−0.077820	0.071440	0.09316	0.1903	0.0612	0.1999
2.20	−0.145040	−0.022280	0.057680	5.0	−0.11753	−0.072670	0.068970	0.09413	0.1897	0.0582	0.1984
2.25	−0.146260	−0.020640	0.053050	5.0	−0.11920	−0.074350	0.069250	0.09749	0.1902	0.0566	0.1984
2.30	−0.159100	−0.017430	0.049370	5.0	−0.11896	−0.073070	0.070840	0.10148	0.1917	0.0527	0.1988
2.35	−0.177910	−0.013600	0.046130	5.0	−0.11843	−0.067850	0.073370	0.09828	0.1929	0.0531	0.2001
2.40	−0.186050	−0.012040	0.043980	5.0	−0.11735	−0.063600	0.075850	0.09863	0.1946	0.0529	0.2017
2.45	−0.182910	−0.013680	0.048380	5.0	−0.11914	−0.062260	0.076620	0.10071	0.1953	0.0543	0.2027
2.50	−0.193310	−0.012690	0.052930	5.0	−0.12100	−0.061320	0.076820	0.10252	0.1954	0.0556	0.2032
2.55	−0.197020	−0.012620	0.056990	5.0	−0.12233	−0.062420	0.076340	0.10285	0.1956	0.0576	0.2039
2.60	−0.198960	−0.012860	0.060750	5.0	−0.12584	−0.063790	0.077800	0.10269	0.1968	0.0579	0.2051
2.65	−0.193450	−0.013880	0.065370	5.0	−0.13307	−0.071880	0.076390	0.11339	0.1971	0.0610	0.2063
2.70	−0.201220	−0.011720	0.066030	5.0	−0.13770	−0.076130	0.075540	0.11532	0.1984	0.0590	0.2070
2.75	−0.204400	−0.011130	0.068520	5.0	−0.14122	−0.077520	0.074810	0.11397	0.1991	0.0573	0.2072
2.80	−0.200780	−0.011490	0.069340	5.0	−0.14548	−0.078790	0.075270	0.11195	0.1997	0.0556	0.2073
2.85	−0.195310	−0.012460	0.070210	5.0	−0.14806	−0.078830	0.075690	0.11258	0.1995	0.0574	0.2076

(*continued*)

Table A2 (*Continued*)

c	b_1	b_2	b_4	b_6	b_7	b_8	b_9	b_{10}	σ_{intra}	σ_{inter}	σ_{total}
2.90	−0.197850	−0.012400	0.073310	5.0	−0.15137	−0.079400	0.075840	0.11443	0.1994	0.0561	0.2071
2.95	−0.197960	−0.012540	0.075530	5.0	−0.15549	−0.080210	0.077000	0.11556	0.1994	0.0548	0.2068
3.00	−0.194310	−0.013020	0.075850	5.0	−0.15830	−0.081210	0.078830	0.11624	0.1993	0.0548	0.2067

2010; Bommer *et al.*, 2007; ITACA [Luzi *et al.*, 2008]; Akkar *et al.*, 2010), number of accelerograms used from each event, and their distance ranges are given in Table A1. Table A2 presents the regression coefficients of the proposed V/H model.

Department of Civil and Environmental Engineering
Imperial College London
South Kensington campus
London
SW7 2AZ
United Kingdom
j.bommer@imperial.ac.uk
(J.J.B.)

Earthquake Engineering Research Center
Department of Civil Engineering
Middle East Technical University
06531 Ankara, Turkey
sakkar@metu.edu.tr
(S.A.)

Department of Civil Engineering
Middle East Technical University
06531 Ankara, Turkey
ozkankale@gmail.com
(Ö.K.)

Manuscript received 12 October 2010